Research Square

Preprints are preliminary reports that have not undergone peer review.
They should not be considered conclusive, used to inform clinical practice,
or referenced by the media as validated information.

Biosourced Natural Latex–Okra Fabric Composites : Processing, Dye-Dependent Properties, and Environmental Aging Response

Solange BASSOK
University of Douala
Ninon Rosine NKOULOU NKOULOU
ninonnkoulou2@gmail.com
University of Douala
Pauline EKALLE LEUPI
University of Douala
Arlette Cécile LISSOM POUGUE
University of Douala
Crépin Constant JOUEYON NGOK
University of Douala
Olivier Thierry SOSSO MAYI
University of Douala
Essiane Salomé NDJACKOMO
University of Douala
Léandre NNEME NNEME
University of Douala
Jean MBIHI
University of Douala

Research Article

Keywords: Okra fibre, natural rubber latex, woven bio-composite, dye-dependent properties, textile reinforcement, environmental ageing

Posted Date: November 11th, 2026

DOI: https://doi.org/10.21203/rs.3.rs-11277848/v1

License: This work is licensed under a Creative Commons Attribution 4.0 International License.
Read Full License

Additional Declarations: No competing interests reported.

Biosourced Natural Latex–Okra Fabric Composites : Processing, Dye-Dependent Properties, and Environmental Aging Response

Solange BASSOK[1,2,3], Ninon Rosine NKOULOU NKOULOU [1,2]*, Pauline EKALLE LEUPI [2,3], Cécile Arlette POUGUE LISSOM[5,6], Crépin Constant JOUEYON NGOK[2,6], Olivier Thierry Sosso Mayi[3,4], Essiane Salomé NDJAKOMO[1,3,4], Léandre NNEME NNEME[1], Jean MBIHI[1,2]

[1] Laboratory of Computer Engineering and Automation, University of Douala, Douala, Cameroon

[2] Textile and Clothing Industries Department, ENSET, University of Douala, P.O. Box: 1872, Douala, Cameroon

[3]Laboratory of Applied Technologies and Sciences (LTSA), University of Douala, Douala, Cameroon

[4]Laboratory of Electronics, Electrical Engineering, Automation and Telecommunications (LEEAT), University of Douala, Douala, Cameroon

[5]Mecanics and Adapted Materials laboratory (LAMMA), Enset, University Of Douala, Cameroon

[6]Mecanic laboratory (LM), Enset, University Of Douala, Cameroon

Corresponding author: Ninon Rosine NKOULOU NKOULOU[1,2]*

ORCID: 0009-0005-6602-1247

Email: ninonnkoulou2@gmail.com

Abstract

Natural-fibre composites with elastomeric matrices offer a promising route toward biosourced, flexible, and water-resistant materials for textile applications. This study investigates a composite combining a woven okra (*Abelmoschus esculentus*) bast-fibre fabric with a natural-rubber latex matrix, produced in red and black dye formulations. Extracted fibres were converted into cohesive Z-twisted cords and manually woven into a plain-weave fabric before latex impregnation. The resulting bio-composites were characterized in terms of physical, mechanical, hydric, morphological, structural, thermal, and colourimetric properties, as well as their response to environmental ageing. Both formulations exhibited 100% water impermeability under the adopted test conditions. Compared with the black formulation, the red bio-composite showed an 87.8% higher Young's modulus and a 64.7% higher maximum stress, together with a 21.5% lower elongation at break and a 21.2% lower water absorption.

The two formulations also exhibited distinct colourimetric characteristics, with a CIE L*a*b* colour difference of approximately ΔE*ab = 28.5. X-ray diffraction confirmed preservation of the cellulose I crystalline structure, while differences in apparent crystallinity were observed between the formulations. Thermal analysis revealed comparable multistage degradation behaviour. After 30 days of environmental ageing, the initial mechanical ranking was not preserved: the black composite retained higher tensile stress after high-humidity exposure, whereas the red formulation retained higher stiffness. Water exposure caused substantial strength losses in both formulations. Overall, the results demonstrate the feasibility of converting okra bast fibres into a functional latex-based textile composite and highlight the importance of considering dye formulation and environmental ageing when assessing its performance for flexible, water-exposed textile applications.

Keywords: Okra fibre; natural rubber latex; woven bio-composite; dye-dependent properties; textile reinforcement; environmental ageing.

1. Introduction

The valorization of underexploited lignocellulosic resources into functional textile reinforcements is an important pathway for expanding the range of biosourced composite materials. Okra (Abelmoschus esculentus) is particularly relevant in this context because its stem contains bast fibres with potential for reinforcement applications. In our previous study, biological, chemical and combined extraction routes were investigated to obtain okra fibres with suitable physicochemical, structural and mechanical characteristics for natural-latex-based composite reinforcement [1]. That work established the material basis for the present study; however, the subsequent conversion of the extracted fibres into a textile reinforcement and its integration into a latex-based composite remain to be addressed.

A major challenge is therefore to transform the extracted fibres into a continuous and sufficiently cohesive textile structure. Twisting provides a practical route for assembling individual plant fibres into continuous load-bearing elements. Rao et al. showed that the behaviour of twisted plant-fibre structures is governed by fibre distribution, porosity and local aggregation [2]. Experimental studies on twisted ramie fibre yarns have similarly demonstrated the influence of twisting on tensile performance and fibre packing [3].

The organization of these twisted structures into a woven reinforcement introduces a further structural scale. Yarn arrangement, fabric density, crimp and cover factor influence reinforcement compactness, matrix impregnation and load transfer. Korkmaz et al. demonstrated that reinforcement architecture can significantly modify the mechanical response of woven composite systems [4]. Kar et al. showed that the configuration of co-woven plant-fibre reinforcements can affect both mechanical and thermal properties [5]. Chowdhury and Summerscales emphasized that woven architecture simultaneously influences permeability, processability and mechanical performance [6]. Anas et al. demonstrated that fabric structure and consolidation conditions can significantly affect the behaviour of cellulose-based composites [7]. Pervaiz et al. further illustrated the importance of woven natural-fibre architecture in textile polymer composites [8]. These findings support the treatment of the okra fabric as a structural component of the composite rather than merely as a carrier for the matrix.

Natural-rubber latex provides an elastomeric matrix particularly suited to flexible composite structures. Omar et al. identified reinforcement morphology, matrix formulation and fibre–matrix interactions among the principal factors governing natural-rubber/natural-fibre composite performance [9]. Li et al. further demonstrated that the internal network structure of natural-rubber-latex-based composites can strongly influence their mechanical response [10].

The development of biosourced alternatives to conventional leather has expanded the application space for plant- and waste-derived materials. Yizengaw et al. reviewed waste-derived leather-like materials and highlighted the potential of agricultural resources for this purpose [11]. Oleksińska-Merida et al. similarly documented the broad range of bio-based and sustainable leather alternatives and the substantial variability of their properties and processing routes [12].

For natural-rubber composites reinforced with cellulose fibres, mechanical and water-related behaviour are closely coupled. Lozada et al. showed that vegetable cellulose fibres modify both the mechanical response and water-transport behaviour of natural-rubber composites, with reinforcement morphology and fibre–matrix interactions playing important roles [13]. This coupling is particularly relevant for flexible textile materials intended for water-exposed environments, where as-produced mechanical properties alone are insufficient to assess functional performance.

A multiscale characterization strategy is consequently required to relate processing and macroscopic performance to the internal structure of the composite. Scanning electron microscopy (SEM) enables examination of fibre embedment, matrix continuity, residual voids and fibre–matrix morphology [14]. Fourier-transform infrared spectroscopy (FTIR) provides complementary information on the principal chemical functionalities of natural fibres and their composites [14]. X-ray diffraction (XRD) enables assessment of cellulose crystalline organization and apparent crystallinity [16]. Thermogravimetric analysis and derivative thermogravimetry (TGA/DTG) provide information on thermal stability and degradation behaviour [17].

Colour is an additional design variable for textile and leather-like materials. The CIE L*a*b* system provides an objective description of lightness and chromatic coordinates, while the CIE 1976 ΔE*ab parameter quantifies the overall colour difference between formulations [18]. In the present study, colourimetric characterization is therefore considered alongside mechanical, hydric and structural characterization rather than as a purely aesthetic assessment.

Despite these advances, an important gap remains. The complete transformation of extracted okra bast fibres into a woven textile reinforcement followed by impregnation with natural-rubber latex has received limited investigation. More importantly, the extent to which dye formulation is associated with differences in mechanical, hydric and other functional properties, and whether these differences remain stable under environmental aging, has not been established for this composite system. Addressing this question requires an integrated experimental approach in which the two formulations are produced through the same processing route and evaluated under comparable conditions.

Accordingly, this study develops biosourced natural latex–okra fabric composites through a hierarchical processing route involving extracted-fibre assembly, Z-twisting, plain weaving and latex impregnation. Red and black formulations are investigated comparatively using physical, mechanical, hydric, morphological, chemical, crystalline, thermal and colourimetric characterization. Their performance is further evaluated after water and high-humidity aging. The study specifically aims to (i) establish a textile processing route for extracted okra fibres; (ii) develop and compare red and black natural-latex/okra-fabric composites; (iii) relate their processing and structural characteristics to their physical, mechanical and functional properties; (iv) determine their response to environmental aging; and (v) identify the potential and limitations of the resulting materials for flexible, water-exposed textile applications.

Importantly, differences between formulations are treated as observed formulation-dependent effects rather than as evidence that the dye itself is the sole causal factor.

2. Materials and Methods

2.1. Materials

The okra bast fibres (Abelmoschus esculentus) used in this study were obtained using the optimized combined biological–alkaline extraction process previously developed by the authors [1]. The selected treatment consisted of 1 wt.% NaOH for 60 min at 50 °C. Following extraction, the fibres were thoroughly washed with distilled water until a near-neutral pH was reached, dried, and conditioned prior to textile processing. Ammonia-stabilized natural rubber latex obtained from Hevea brasiliensis was used as the polymeric matrix. The ammonia stabilizer was retained to preserve latex colloidal stability during handling and processing. Red and black dyes were incorporated into the latex formulations to produce two bio-composite variants and to investigate the influence of formulation on the resulting physical, mechanical, and functional properties.

2.2. Preparation and characterization of twisted okra-fibre cords

2.2.1. Preparation of twisted okra-fibre cords

Following extraction, the okra fibres were opened, individualized, aligned, and prepared for textile processing. Preliminary trials using conventional spinning resulted in repeated fibre breakage and separation of the fibre bundle. Consequently, a manual twisting procedure was adopted to preserve fibre integrity and obtain continuous textile elements suitable for weaving. The aligned fibres were manually twisted in the Z direction until continuous and sufficiently cohesive cords were obtained. The twisting operation was continued until an average cord diameter of approximately 0.5 cm was achieved. The resulting twisted cords were subsequently characterized in terms of linear density, diameter, cross-sectional area, tensile strength, tenacity, packing coefficient, porosity, moisture regain, and water absorption.

2.2.2. Characterization of the twisted cords

1. Linear density

The linear density of the twisted cords was determined according to:

$$\boldsymbol{Tex = \frac{m \times 1000}{L}} \quad \textbf{(1)}$$

Where is the linear density (tex), is the cord mass (g), and is the cord length (m).

2. Equivalent diameter

The equivalent diameter of the cord was determined from its mass, length, and apparent density:

$$d = \sqrt{\frac{4m}{\pi \rho L}} \quad (2)$$

Where is the equivalent cord diameter, is the cord mass, is the apparent cord density, and is the cord length. The experimentally obtained mean diameter used for subsequent textile calculations was 0.5 cm.

3. Cross-sectional area

Assuming an approximately circular equivalent cross-section, the cross-sectional area was calculated as:

$$A = \frac{\pi d^2}{4} \quad (3)$$

Where is the cross-sectional area (mm^2) and is the equivalent diameter (mm).

4. Tensile stress

The tensile stress at failure was calculated from the breaking force and the initial cross-sectional area:

$$\sigma = \frac{F}{A} \quad (4)$$

Where is the tensile force (N), is the initial cross-sectional area (mm^2), and is the tensile stress (MPa).

1. Tenacity

The cord tenacity was calculated independently from the breaking force and linear density:

$$T = \frac{F_{break}}{Tex} \quad (5)$$

Where is the tenacity (cN/tex) and F_{break} is the breaking force expressed in centinewtons.

2. Cord compactness

The compactness of the twisted cord was estimated from the ratio between its apparent density and the density of the extracted fibre:

$$K = \frac{\rho_{cord}}{\rho_{fibre}} \quad (6)$$

Where K is the cord compactness.

3. Cord porosity

The internal porosity of the twisted cord was estimated from its apparent density relative to the reference density of cellulose:

$$P(\%) = \left(1 - \frac{\rho_{cord}}{\rho_{ref}}\right) \times 100 \quad (7)$$

Where P is the estimated porosity and is the reference density of cellulose. Accordingly, this parameter is considered an **estimated structural porosity**, rather than a direct measurement of the internal void volume.

4. Moisture regain and water absorption

The moisture regain and water absorption of the twisted cords were estimated from the corresponding properties of the extracted fibres using structural correction coefficients:

$$MR_{cord}(\%) = k_{MR} \times MR_{fiber} \quad (8)$$
$$WA_{fil}(\%) = k_{WA} \times WA_{fiber}$$

Where and are correction coefficients associated with the twisted-cord structure. The characterized cords were subsequently used as warp and weft elements for fabric production.

2.3. Fabrication of the woven okra-fibre reinforcement

The twisted okra-fibre cords were used as both warp and weft elements to manufacture the textile reinforcement. A plain-weave architecture (1/1) was selected because of its simple and stable interlacing configuration and its high number of warp–weft interlacing points. This architecture was considered suitable for subsequent impregnation with natural-rubber latex. The fabric was manually produced on a traditional loom measuring 2.00 m × 0.65 m. The warp cords were first arranged under tension and regularly distributed across the loom width. The weft cords were subsequently inserted perpendicular to the warp and manually interlaced according to the 1/1 plain-weave pattern. The resulting fabric was subsequently conditioned

and characterized before composite fabrication. The manufacturing process of the woven okra-fibre fabric is illustrated in Figure 1.

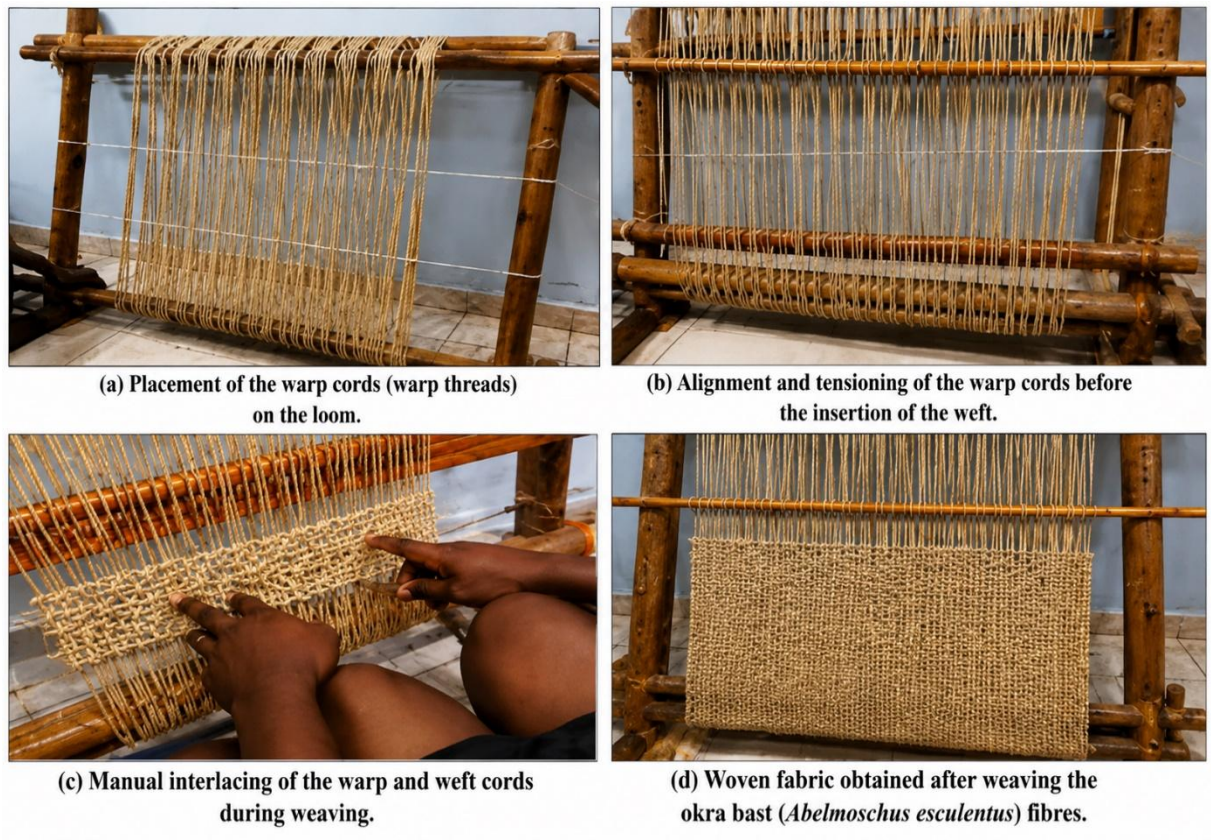


Figure 1. *Manufacturing process of the woven okra-fibre fabric (Abelmoschus esculentus) by manual plain weaving: (a) placement of the warp cords on the loom; (b) alignment and tensioning of the warp cords before weft insertion; (c) manual interlacing of the warp and weft cords during weaving; and (d) woven fabric obtained after weaving the okra bast fibres.*

2.4. Textile architecture characterization

The principal architectural parameters of the woven reinforcement were determined from the fabric geometry.

The fabric dimensions were:

1. fabric width: **60 cm**;
2. fabric length: **2.00 m**;
3. number of warp cords: **140**;
4. number of weft cords: **110**;
5. mean cord diameter: **0.5 cm**;
6. weave structure: **plain weave (1/1)**;
7. estimated weft crimp: **12%**.

Warp density

$$\mathbf{D_w = \frac{N_w}{W}} \quad (\mathbf{9})$$

Where : D_w is the warp density (cords·cm), N_w is the number of warp cords, and W is the fabric width (cm).

Weft density

$$\boldsymbol{D_f = \frac{N_f}{W}} \quad (\mathbf{10})$$

Where D_f: is the weft density (cords·cm) and N_f: is the number of weft cords.

Binding ratio

For the plain-weave structure, the binding ratio was calculated as:

$$\boldsymbol{R_b = \frac{n_o}{n_o + n_u}} \quad (\mathbf{11})$$

Where n_o and n_u represent the numbers of over- and under-crossings, respectively. For an ideal 1/1 plain weave, the theoretical binding ratio is 0.5.

Weft crimp

The weft crimp was calculated as:

$$C_f = \frac{L_f - L_0}{L_0} \times 100 \quad (12)$$

Where L_f is the actual length of the weft cord and is L_0 its projected length.

Warp and weft cover factors

The warp and weft cover factors were estimated according to:

$$C_w = D_w \cdot d \quad (13)$$

$$C_f = D_f \cdot d \quad (14)$$

Where d is the mean cord diameter.

Total cover factor

$$C_t = C_w + C_f \quad (15)$$

The calculated cover factors were used to describe the relative degree of yarn packing within the textile structure.

Estimated geometrical porosity

Because cover factor is not itself a direct measurement of void fraction, the resulting open structure was described as an estimated geometrical porosity rather than a directly measured porosity. Where the adopted geometrical approximation is used, it is expressed as:

$$P_{geo} = 1 - C_t \quad (16)$$

This parameter is therefore interpreted only as an approximation of the open area and should not be considered equivalent to experimentally measured three-dimensional porosity.

Warp–weft contact-point density

The theoretical density of warp–weft intersections was calculated as:

$$N_c = D_w \cdot D_f \quad (17)$$

Where is the contact-point density (contacts·cm).

Fibre volume fraction

For the final composite, the fibre volume fraction was estimated from the respective masses and densities of the reinforcement and matrix:

$$V_f = \frac{m_f/\rho_f}{(m_f/\rho_f)+(m_m/\rho_m)} \quad (18)$$

Where $\boldsymbol{m_f}$ and $\boldsymbol{m_m}$ are the fibre and matrix masses, respectively, and and are their corresponding densities.

2.5. Mechanical characterization of the woven reinforcement

2.5.1. Thickness and areal density

Rectangular fabric specimens measuring 100 × 50 mm, corresponding to an area of 0.005 m², were prepared. The specimen thickness was measured at several locations using a digital micrometer, and the mean value was used as the representative thickness. The specimens were subsequently weighed using a precision balance. The areal density was calculated as:

$$\boldsymbol{G = \frac{m}{A}} \qquad (\mathbf{19})$$

Where $\boldsymbol{G}$ is the areal density ($g \cdot m^{-2}$), $\boldsymbol{m}$ is the specimen mass (g), and A is the specimen area (m^2). The procedure used to determine the specimen dimensions, thickness, and mass is illustrated in Figure 2.

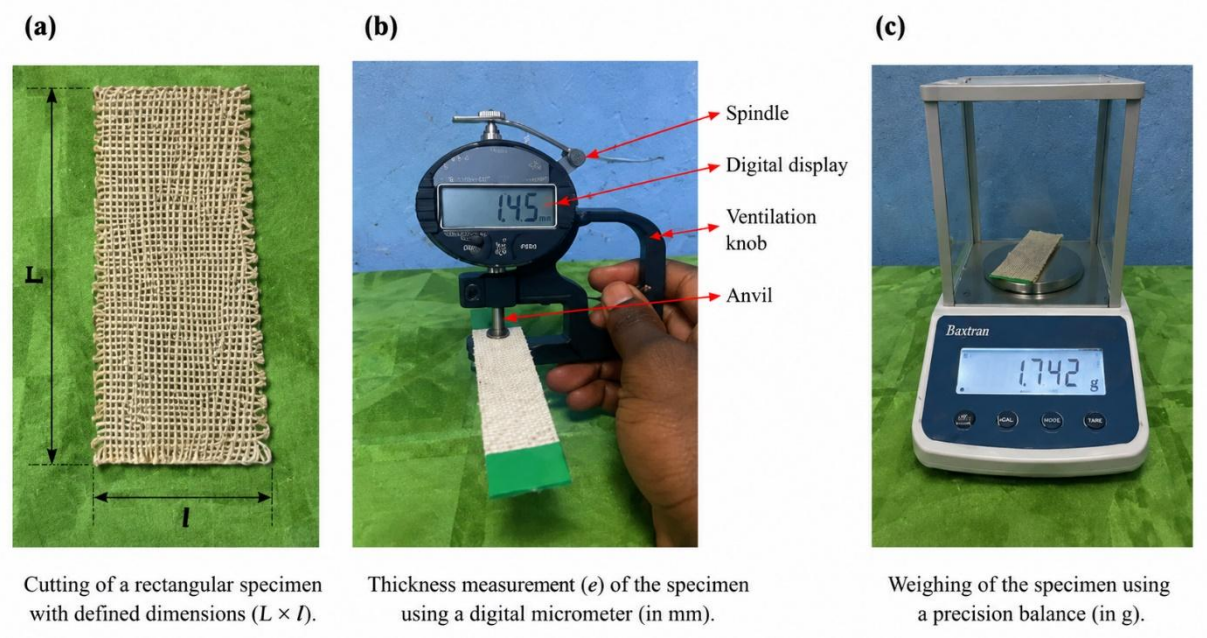


Figure 2. *Experimental procedure for determining the dimensions, thickness, and mass of the woven okra-fibre fabric specimens.* **(a)** Cutting of a rectangular specimen with defined dimensions . **(b)** Thickness measurement of the specimen using a digital micrometer (mm).**(c)** Determination of specimen mass using a precision balance (g).

2.5.2. Tensile characterization of the woven fabric

The tensile properties of the woven okra-fibre reinforcement were determined by uniaxial tensile testing according to ISO 13934-1. The tests were performed using a COYON CJ-0820 universal testing machine. The crosshead speed was set to 5 m/min, according to the experimental protocol. Prior to testing, the specimens were dried at 105 °C for at least 12 h and subsequently conditioned at 65% relative humidity for 24 h. The specimens were mounted between the grips with their longitudinal axis aligned with the loading direction.The initial gauge length was 200 mm. This value is now used consistently throughout the tensile analysis. The maximum tensile stress was calculated according to:

$$\boldsymbol{\sigma_{max} = \frac{F_{max}}{S}} \quad (\mathbf{20})$$

Where $\boldsymbol{F_{max}}$ is the maximum tensile force and $\boldsymbol{S}$ is the initial cross-sectional area.

The strain at break was calculated as:

$$\boldsymbol{\varepsilon_{break} = \frac{\Delta L_{break}}{L_0}} \quad (\mathbf{21})$$

Where $\boldsymbol{\Delta L_{break}}$ is the elongation at break and L_0= 200 mm.

The apparent Young's modulus was obtained from the slope of the linear portion of the stress–strain curve:

$$\boldsymbol{E = \frac{\sigma_2 - \sigma_1}{\varepsilon_2 - \varepsilon_1}} \quad (\mathbf{22})$$

The preparation, conditioning, and tensile characterization procedure is shown in Figure 3.

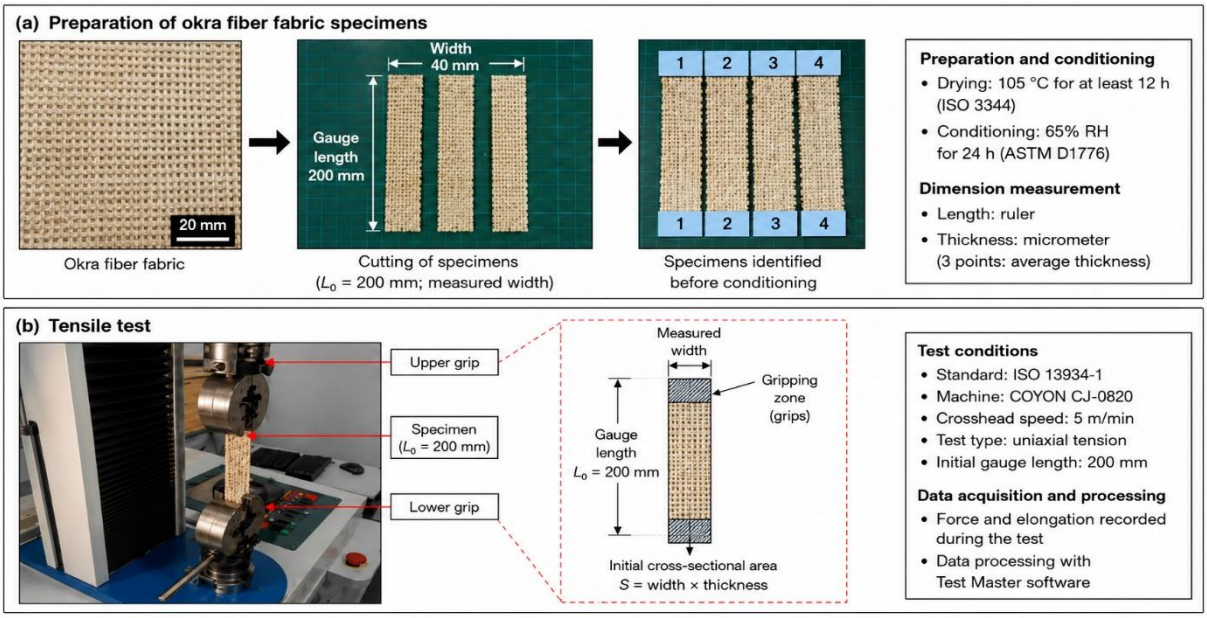


Figure 3. *Preparation, conditioning, and tensile testing of woven okra-fibre fabric specimens. (a) Preparation of okra-fibre fabric specimens: fabric, cutting of specimens with a 200 mm gauge length and measured width, specimen identification, drying, conditioning, and dimensional measurements. (b) Uniaxial tensile testing: specimen mounting between the upper and lower grips, specimen geometry and initial cross-sectional area, test conditions, and force–elongation data acquisition and processing.*

2.6. Characterization of the natural-rubber latex

2.6.1. Total solids content

The total solids content (TSC) of the natural-rubber latex was determined gravimetrically. A clean and dry crucible was first weighed to obtain . A known amount of latex was then introduced into the crucible, and the assembly was weighed to obtain . The sample was dried until constant mass, after which the crucible containing the dried solids was weighed to obtain The total solids content was calculated as:

$$\mathbf{TSC}\ (\%) = \frac{(\boldsymbol{m_2} - \boldsymbol{m_0})}{(\boldsymbol{m_1} - \boldsymbol{m_0})} * \mathbf{100} \qquad (\mathbf{23})$$

Where $\boldsymbol{m_0}$ is the mass of the empty crucible, $\boldsymbol{m_1}$ is the mass of the crucible plus wet latex, and $\boldsymbol{m_2}$ is the mass of the crucible plus dried solids. Measurements were performed in duplicate, and the mean value was reported.

2.6.2. Latex viscosity

The dynamic viscosity of the latex was determined using an Ubbelohde viscometer, with distilled water used as the reference fluid. The dynamic viscosity was calculated as:

$$\eta_{latex} = \frac{(\eta_{water} * \rho_{latex} * t_{latex})}{\rho_{water} * t_{water}} \quad (24)$$

Where η is the dynamic viscosity, ρ is density, and t is flow time. Measurements were performed under controlled temperature conditions.

2.6.3. Latex density

The density of the latex was determined from the mass of a known volume:

$$\rho_{latex} = \frac{m_1 * m_0}{v} \quad (25)$$

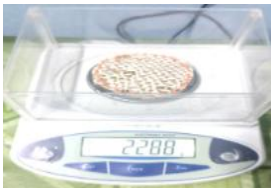
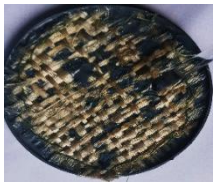
Where m_0 is the mass of the empty container, m_1 is the mass of the container filled with latex, and v is the latex volume.

2.7. Fabrication of the latex/okra-fibre bio-composites

The woven okra-fibre fabric was used as the reinforcement, while natural-rubber latex served as the continuous polymeric matrix.

The fabric specimens were first cut to the required dimensions, and their edges were sewn to minimize fraying during handling and impregnation. The specimens were weighed before impregnation. Preliminary trials were conducted to determine an adequate quantity of latex for complete wetting of the textile structure. For each formulation, the natural-rubber latex was mixed with the corresponding red or black powder dye. The mixture was manually stirred for approximately **1 min** to promote homogeneous dispersion of the dye. The resulting latex–dye formulation was applied to the woven okra-fibre fabric until impregnation was achieved. The impregnated specimens were then allowed to dry under ambient conditions for **three days**. After drying, the resulting bio-composites were conditioned before characterization. The manufacturing procedure used to produce the red and black latex/okra-fibre bio-composites is summarized in Table 1.

Table 1. *Manufacturing procedure used for the red and black latex/okra-fibre bio-composites.*

Step	Procedure	Images
1	Cut and prepare the woven fabric specimens and sew the edges.	
2	Weigh the fabric specimens before impregnation.	
3	Measure the required volume of natural-rubber latex.	 
4	Weigh the red or black dye. Mix the dye with the latex for approximately 1 min.	 
6	Impregnate the woven okra-fibre reinforcement with the corresponding formulation.	 

7 Allow the impregnated material to dry for three days under ambient conditions.





8 Condition the resulting bio-composites before characterization.





2.7.1. Interfacial interactions and composite formation

The alkaline treatment applied during fibre extraction modifies the lignocellulosic structure by removing part of the non-cellulosic constituents and altering the fibre surface [1]. During composite fabrication, the natural-rubber latex penetrates the inter-yarn spaces of the woven reinforcement and forms the continuous polymeric phase after drying. The resulting composite structure is expected to be governed by a combination of mechanical interlocking, physical interactions, fibre wetting, and interfacial adhesion between the lignocellulosic reinforcement and the natural-rubber matrix.The red and black dyes were considered formulation components and were incorporated into the latex before impregnation. Because no dedicated spectroscopic or surface-chemical characterization was performed to directly

identify covalent bonding between cellulose, dye, and natural rubber, specific chemical reactions are not assigned as experimentally demonstrated mechanisms in the present study. This formulation is scientifically safer and avoids overclaiming the formation of specific chemical bonds.

2.8. Characterization of the bio-composites

The red and black bio-composites were characterized in terms of their physical, hydric, mechanical, and environmental behaviour. The woven okra-fibre reinforcement constituted the l trix. 2.8.1 ISO 4920 at a distar ntal. Each face of th ntal setup

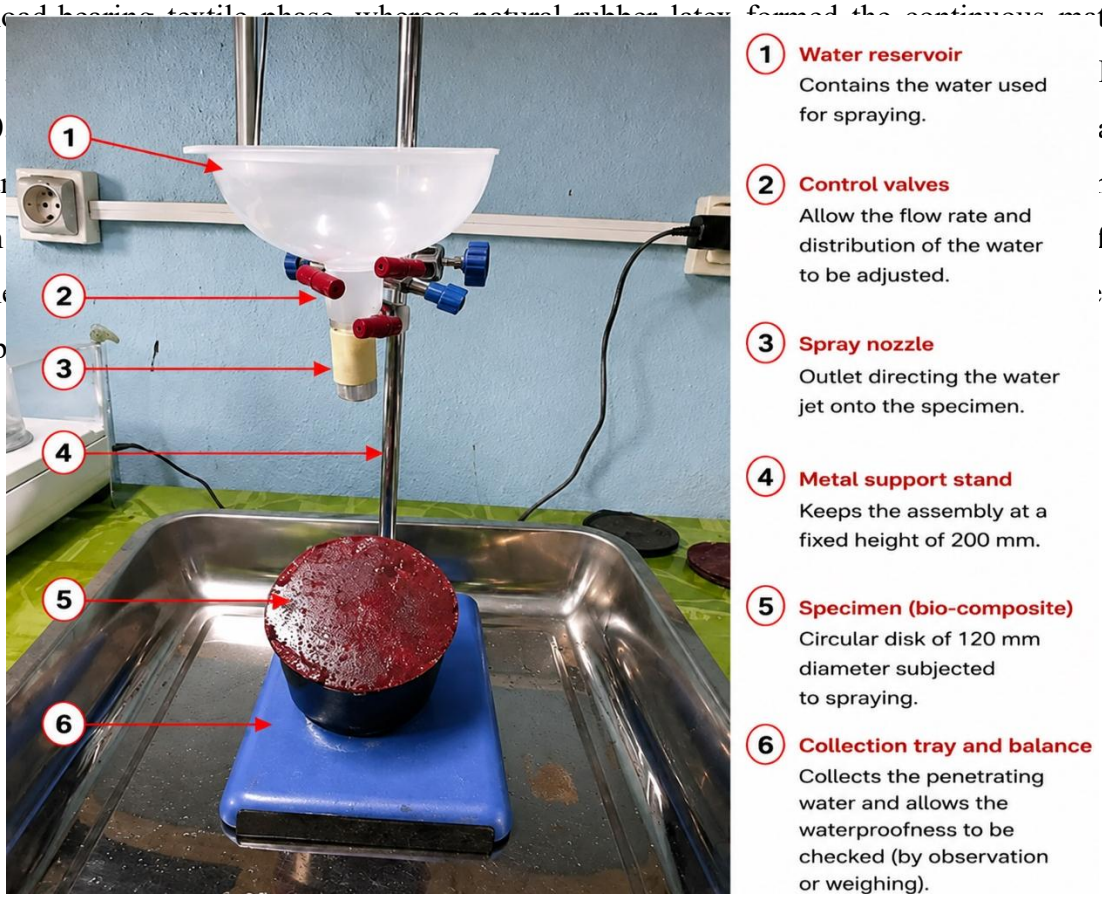


Figure 4. *Experimental setup for evaluating the waterproofness of the developed bio-composites by spray testing: (1) water reservoir; (2) control valves; (3) spray outlet; (4) metal support; (5) bio-composite specimen; and (6) collection tray.*

2.8.2. Areal density

Square specimens measuring 20 × 20 mm were dried at 60 °C for 12 h and subsequently conditioned for 24 h at 65% relative humidity. The specimens were weighed using a precision balance with a resolution of 0.001 g. The areal density was calculated as equation (19).

2.8.3. Thickness

The thickness of the bio-composite specimens was measured after drying and conditioning. Five measurements were taken at different locations on each specimen using a micrometer. The arithmetic mean was reported as the representative thickness.

2.8.4. Moisture regain

Moisture regain was determined according to **ISO 483:2005**. The moisture regain was calculated as:

$$\mathbf{M}_{\boldsymbol{R}} = \frac{\mathbf{m_f - m_i}}{\mathbf{m_i}} * \mathbf{100} \qquad (\mathbf{26})$$

Where $\mathbf{m_i}$ is the initial dry mass and $\mathbf{m_f}$ is the mass after conditioning.

2.8.5. Water absorption

Water absorption was calculated from the dry and saturated masses:

$$\boldsymbol{WA}(\%) = \frac{\mathbf{m_{sss} - m_0}}{\mathbf{m_0}} * \mathbf{100} \qquad (\mathbf{27})$$

Where $\mathbf{m_0}$ is the initial dry mass and $\mathbf{m_{SSS}}$ is the saturated surface-dry mass.

2.8.6. Environmental ageing

To investigate the influence of environmental exposure on the mechanical behaviour of the bio-composites, the specimens were divided into three groups: ENV (unaged reference specimens), EVE (water-aged specimens), and EVH (high-humidity-aged specimens).

The EVE specimens were immersed in distilled water. The EVH specimens were exposed to an atmosphere of approximately 98% relative humidity, generated using a saturated K_2SO_4 solution. Both ageing conditions were maintained for 30 days. [Correction: missing space] The ENV specimens were maintained under reference conditioning conditions without accelerated ageing. Following exposure, the aged specimens were removed from their respective environments and prepared for tensile characterization. The mechanical tests were conducted using a universal testing machine with a 5 kN load capacity at a crosshead speed of 5 mm/min. [Correction: missing space] The resulting force–displacement curves were used to determine the maximum tensile stress, apparent Young's modulus, and strain at break. The responses of the ENV, EVE, and EVH groups were compared to assess the effects of water and high-humidity exposure on the mechanical stability of the bio-composites. The environmental ageing conditions and post-ageing tensile testing are illustrated in Figure 5.

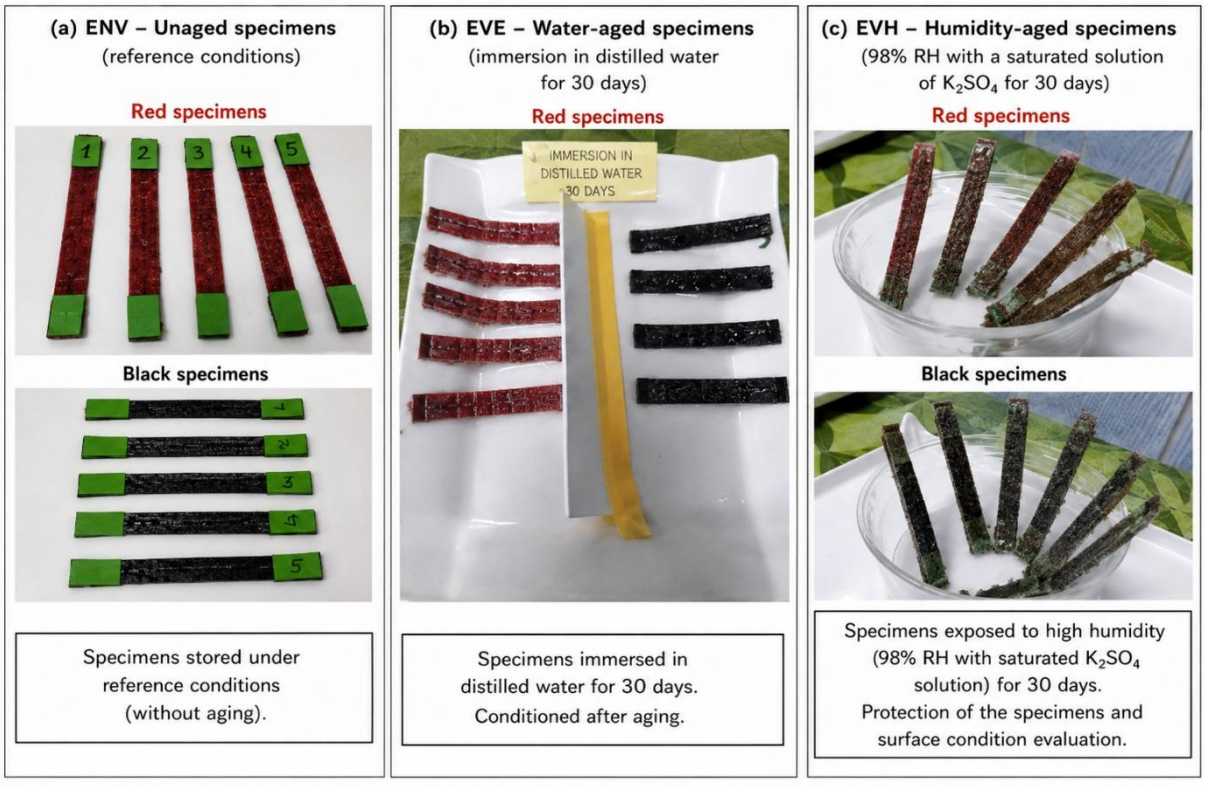


Figure 5. *Bio-composite specimens subjected to different environmental ageing conditions: (a) unaged specimens (ENV); (b) water-aged specimens (EVE); (c) high-humidity-aged specimens (EVH); and (d) tensile testing after ageing.*

2.8.7. Tensile characterization of the bio-composites

The tensile properties of the bio-composites were determined by uniaxial tensile testing in accordance with ISO 13934-1. The specimens were prepared with a nominal width of 20 mm and an approximate thickness of 0.95 mm. The initial gauge length was set according to the experimental protocol used for the bio-composite specimens. Prior to testing, the specimens were dried at 105 °C for 6 h and subsequently conditioned for 24 h at 65% relative humidity. The specimens were mounted between the grips of the universal testing machine, with their longitudinal axis carefully aligned with the loading direction to minimize misalignment and slippage. Tensile loading was applied at a crosshead speed of 5 mm/min until failure, while force and elongation were continuously recorded. The resulting stress–strain curves were processed using Test Master software to determine the maximum tensile force, maximum tensile stress, strain at break, and apparent Young's modulus. The resulting stress–strain curves were processed using Test Master software to determine:

1. maximum tensile force;
2. maximum tensile stress;
3. strain at break;
4. apparent Young's modulus.

The maximum tensile stress was calculated as equation (20), (21), (22).

While the physical, mechanical, hydric and durability characterizations provide information on the macroscopic performance of the developed bio-composites, these properties are intrinsically related to their microstructural organization and fibre–matrix interactions. Therefore, complementary morphological characterization was performed by scanning electron microscopy (SEM) to examine the matrix continuity, fibre embedment, interfacial morphology and residual porosity of the red- and black-dyed bio-composites.

2.8.8. Scanning electron microscopy (SEM)

The morphology of the red- and black-dyed okra-fibre/natural-latex bio-composites was examined using scanning electron microscopy (SEM) to characterize the surface morphology, fibre–matrix interface, matrix continuity and apparent porosity. SEM observations were performed in secondary electron imaging (SEI) mode at an accelerating voltage of 10 kV. Micrographs were acquired at magnifications of ×200, ×500, ×1,000 and ×2,000, with working distances ranging from 10.1 to 10.3 mm.

The bio-composite specimens were prepared prior to SEM observation to obtain representative observation surfaces. Particular attention was given to the morphology of the latex matrix surrounding the woven okra-fibre reinforcement and to the presence of interfacial discontinuities, exposed fibre regions and voids. The red- and black-dyed formulations were examined under comparable imaging conditions to enable qualitative morphological comparison.

The SEM micrographs were subsequently analysed qualitatively to identify differences in matrix continuity, fibre embedment and apparent interfacial morphology between the two formulations. These observations were used to support the interpretation of the mechanical behaviour of the bio-composites.

Fourier-transform infrared spectroscopy (FTIR) was used to characterize the chemical structure of the developed red- and black-dyed okra-fibre/natural-latex bio-composites. The analysis was performed to identify the main functional groups associated with the lignocellulosic fibre reinforcement and the natural-latex matrix and to compare the infrared spectral profiles of the two dyed formulations.

2.8.9. Fourier-transform infrared spectroscopy (FTIR)

Fourier-transform infrared spectroscopy (FTIR) was used to characterize the chemical structure of the red- and black-dyed okra-fibre/natural-latex bio-composites and to identify the main functional groups associated with the lignocellulosic fibre and natural-latex matrix.

The FTIR spectra were recorded over the 4000–400 cm^{-1} wavenumber range in transmittance mode. The spectra were acquired for both the red- and black-dyed bio-composite formulations under identical measurement conditions to enable direct comparison of their characteristic absorption bands.

The main absorption bands were identified from their corresponding wavenumbers and assigned to the functional groups associated with the cellulose-rich fibre phase and the natural-latex (polyisoprene) matrix. Particular attention was given to the characteristic O–H, C–H, C=C, C–O–C and C–O vibrational bands. The positions of the principal bands were subsequently used for comparison between the two formulations. The experimental conditions used for the FTIR measurements are summarized in Table 2.

Table 2. *Experimental conditions used for FTIR analysis*

Parameter	Experimental condition
Technique	Fourier-transform infrared spectroscopy (FTIR)
Spectral range	4000–400 cm^{-1}
Measurement mode	Transmittance
Samples	Red- and black-dyed okra-fibre/natural-latex bio-composites
Spectral analysis	Identification and assignment of characteristic absorption bands

2.8.10. X-ray diffraction (XRD)

X-ray diffraction (XRD) analysis was performed to investigate the crystalline structure of the red- and black-dyed okra-fibre/natural-latex bio-composites and to assess differences in their degree of structural organization.

The diffraction patterns were recorded under identical experimental conditions for both bio-composite formulations. The main diffraction reflections were identified from their corresponding positions and assigned to the crystalline planes of the cellulose-rich reinforcement based on their characteristic diffraction features.

The apparent crystallinity index (CrI) was estimated using the empirical Segal method:

where is the intensity of the principal crystalline cellulose reflection and is the intensity corresponding to the amorphous contribution.

The diffraction profiles were subsequently compared in terms of peak position, relative intensity and apparent crystallinity to evaluate differences in the crystalline organization of the red- and black-dyed bio-composites.

2.8.11. Thermogravimetric analysis (TGA/DTG)

Thermogravimetric analysis (TGA) and derivative thermogravimetric analysis (DTG) were performed to investigate the thermal stability and degradation behaviour of the red- and black-dyed okra-fibre/natural-latex bio-composites. The analyses were carried out using a NETZSCH STA 449 F3 simultaneous thermal analyzer under a nitrogen (N_2) atmosphere.The experimental conditions used for the TGA/DTG measurements are summarized in Table 3.

Table 3. *Experimental conditions used for TGA/DTG analysis*

Parameter	Experimental condition

Instrument	NETZSCH STA 449 F3
Atmosphere	Nitrogen (N_2)
Nitrogen flow rate	50 mL/min
Sample mass	Approximately 10 mg
Crucible	Al_2O_3
Temperature range	25–800 °C
Heating rate	10 °C/min
Analysis	TGA and DTG

Approximately 10 mg of each bio-composite sample was placed in an Al_2O_3 crucible and heated from 25 to 800 °C at a constant heating rate of 10 °C/min, under a nitrogen flow of 50 mL/min. The TGA curves were used to monitor the variation in sample mass as a function of temperature, whereas the DTG curves were obtained from the first derivative of the mass-loss curve with respect to temperature.

The main degradation stages were subsequently identified from the TGA profiles, while the corresponding maximum degradation temperatures (DTG peaks) were determined from the DTG curves. The residual mass at 800 °C was also recorded for comparison of the thermal decomposition behaviour of the red- and black-dyed bio-composites.

2.8.12. Colorimetric characterization of the bio-leathers

The colour properties of the developed bio-leathers were characterized using the **CIE L*a*b*** colour space. The measurements were performed on the black- and red-dyed bio-leathers prepared from okra-fibre fabric and natural latex. The experimental measurement of the CIE L*a*b* colour coordinates using the 3NH NR10QC colorimeter is illustrated in Figure 6.

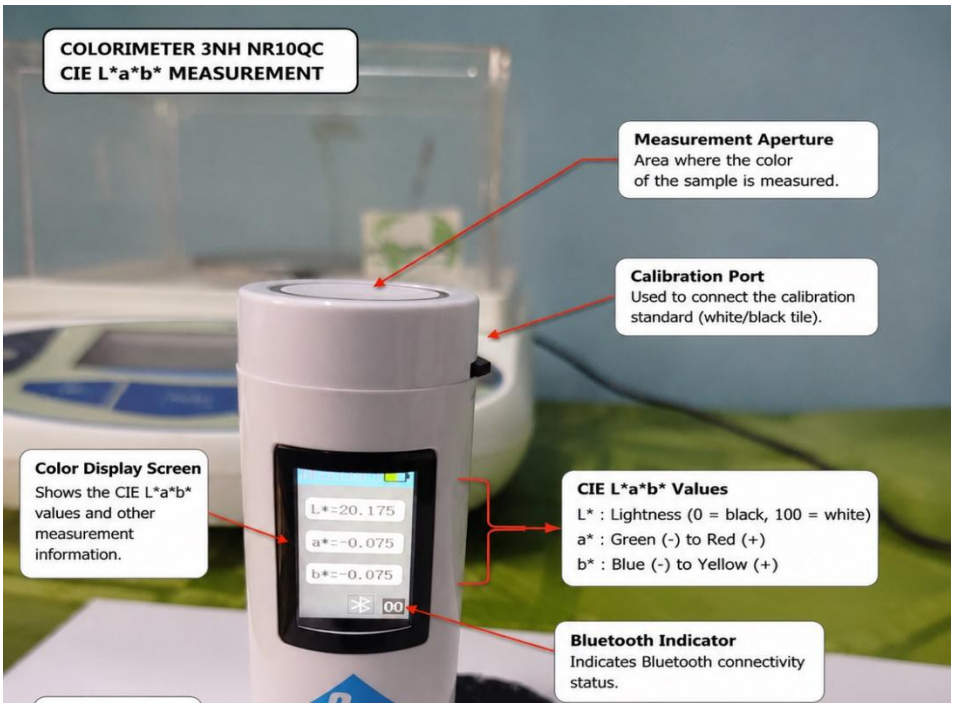


Figure 6. *Experimental measurement of the CIE L*a*b* colour coordinates of the bio-leather using a 3NH NR10QC colorimeter.*

The colour of each bio-leather was characterized using the three CIE L*a*b* coordinates. The **L*** coordinate represents lightness, with values ranging from black to white, whereas **a*** represents the green–red chromatic axis and **b*** represents the blue–yellow chromatic axis. The colour coordinates were recorded for the two formulations under identical measurement conditions.

The colour difference between the black and red bio-leathers was determined using the **CIE 1976 colour-difference equation**, , calculated as the Euclidean distance between the two colour coordinates in the CIE L*a*b* colour space:

$$\Delta E^*_{ab} = \sqrt{(L^*_2 - L^*_1)^2 + (a^*_2 - a^*_1)^2 + (b^*_2 - b^*_1)^2}$$

Where L^*_1 , a^*_1, b^*_1 correspond to the black bio-leather and L^*_2 , a^*_2, b^*_2 correspond to the red bio-leather.

The obtained **L***, **a*** and **b*** coordinates were subsequently used to compare the colour characteristics of the two bio-leather formulations, while the calculated ΔE^*_{ab} value was used to quantify the overall colour difference between the black and red materials.

3. RESULTS AND DISCUSSION

3.1. Physicomechanical properties of twisted okra-fibre cords

The conversion of *Abelmoschus esculentus* bast fibres into a continuous textile reinforcement is a critical step in the development of the proposed bio-composite. The properties obtained for the cords produced by manual twisting in the Z direction are presented in Table 4.

Table 4. *Physical and mechanical properties of the twisted okra-fibre cords*

Characterized property	Symbol	Unit	Value
Mean cord diameter	d	cm	0.50 ± 0.02
Linear density	Tex	tex	15,000 ± 800
Apparent density	ρcord	g/cm³	0.95 ± 0.04
Fibre density	ρfibre	g/cm³	1.45 ± 0.05
Cross-sectional area	A	mm²	19.63 ± 1.50
Maximum breaking force	F	N	750 ± 40
Breaking stress	σ	MPa	38.2 ± 2.5
Elongation at break	ε	%	4.8 ± 0.5
Tenacity	T	cN/tex	5.0 ± 0.3
Packing coefficient	K	–	0.66 ± 0.03
Structural porosity	P	%	34.5 ± 2.0
Moisture regain	MR	%	7.0 ± 0.4
Water absorption	WA	%	45 ± 3
Twist direction	–	–	Z
Weavability	–	–	Good cohesion, no fibre separation

The resulting cord exhibited a mean diameter of 0.50 ± 0.02 cm and a linear density of 15,000 ± 800 tex. These values characterize a cord-like structure rather than a conventional textile yarn. The relatively large cross-section results from the bundling of a substantial number of elementary fibres, which was necessary because conventional spinning did not provide sufficient cohesion for the extracted okra fibres. The significance of this transformation therefore does not lie in producing a fine yarn in the conventional textile sense, but rather in generating a continuous reinforcement element capable of maintaining its structural integrity under mechanical loading. Twisting imposes a collective organization on the elementary

fibres and increases frictional interactions between them. Consequently, relative fibre slippage is restricted and a larger fraction of the constituent fibres can be mobilized simultaneously under load. This behaviour is consistent with the work of Rao et al. [1], who demonstrated that the mechanical response of twisted fibre structures depends on their hierarchical organization, porosity and local aggregation effects. Maidina et al. [2] likewise showed that twisting modifies the tensile behaviour of natural-fibre yarns through interactions among the constituent fibres. The apparent density of the cord was 0.95 ± 0.04 g/cm³, compared with 1.45 ± 0.05 g/cm³ for the individual fibre. The resulting ratio gives a packing coefficient of 0.66 ± 0.03. This value indicates partial consolidation of the fibre bundle while preserving inter-fibre voids. The measured porosity of 34.5 ± 2.0% confirms this structural organization. This feature has a dual implication for composite processing. A sufficiently large inter-fibre volume may facilitate matrix penetration into the reinforcement. Conversely, unfilled voids remaining after consolidation could act as structural defects and reduce the efficiency of stress transfer. Initial porosity should therefore not be regarded as intrinsically beneficial or detrimental. Its relevance depends on the ability of the impregnation process to convert the accessible inter-fibre volume into matrix-filled volume. This relationship between porosity, fibre organization and load transfer is also consistent with the observations reported by Rao et al. [1]. Mechanically, the twisted cord reached a maximum force of 750 ± 40 N, corresponding to a breaking stress of 38.2 ± 2.5 MPa, a tenacity of 5.0 ± 0.3 cN/tex, and an elongation at break of 4.8 ± 0.5%. The combination of relatively high breaking stress and limited elongation indicates that the twisted structure can withstand the mechanical stresses imposed during weaving while maintaining moderate deformability. However, the measured strength represents the collective response of the twisted structure and should not be directly interpreted as the intrinsic strength of an individual fibre. It depends simultaneously on the number of constituent fibres, fibre orientation, twist level, frictional interactions and load redistribution within the cord. Twisting therefore acts as a mechanical cohesion mechanism. When a load is applied, the constituent fibres are not loaded independently; inter-fibre interactions promote stress redistribution and limit fibre separation. This interpretation is consistent with the observations of Maidina et al. [2]. The moisture regain and water absorption values were 7.0 ± 0.4% and 45 ± 3%, respectively. These values confirm the hydrophilic nature of the lignocellulosic reinforcement. This characteristic may facilitate initial wetting of the reinforcement during latex impregnation, but it may also contribute to environmental moisture exchange during subsequent ageing of the composite.

Overall, the results establish the first level of the structure–property relationship of the system: twisting converts the elementary okra fibres into a continuous reinforcement with a balance between cohesion, mechanical strength, packing and inter-fibre accessibility. This structure provides the basis for the textile architecture subsequently used to manufacture the bio-composite.

3.2. Characteristics of the natural rubber latex and impregnation capability

3.2.1. Total solids content

The total solids content of the latex was 47.07% for the first sample and 46.69% for the second sample, giving an average value of 46.88%. This value indicates that a substantial fraction of the initial formulation corresponds to material capable of contributing to the formation of the polymeric network after removal of the aqueous phase. For the proposed bio-composite, the total solids content is an important formulation parameter because the matrix must simultaneously coat the fibre elements, fill the inter-fibre spaces and provide continuity of the polymeric phase after drying. However, solids content cannot be interpreted independently of viscosity and reinforcement architecture. A relatively high solids content will not necessarily result in effective impregnation unless the matrix also possesses sufficient mobility to penetrate the accessible volume of the textile reinforcement.

3.2.2. Latex viscosity

The dynamic viscosity of the natural-rubber latex, determined using an Ubbelohde viscometer, was 1.14 mPa·s. The measured flow times were 125 s for the latex and 111 s for distilled water. The corresponding densities used in the viscosity calculation were 1.0093 g/cm³ for the latex and 0.998 g/cm³ for water, respectively. The latex density of 1.0093 g/cm³ corresponds to the mean of three independent measurements (1.0006, 1.0116, and 1.0156 g/cm³). The relatively low viscosity indicates that the latex matrix remained sufficiently fluid under the experimental conditions to facilitate impregnation of the woven reinforcement. This characteristic is particularly relevant considering the architecture of the okra-fibre fabric, which contains interconnected inter-fibre spaces that can potentially be infiltrated by the polymeric phase. The relationship between matrix viscosity and reinforcement architecture is therefore an important parameter governing the processing route. A sufficiently mobile latex can penetrate the inter-fibre and inter-yarn spaces before drying, whereas incomplete impregnation may result in fibre-rich/matrix-poor regions and local heterogeneities. In a natural-rubber-based composite, such heterogeneity may impair stress-transfer continuity and

promote local stress concentrations, thereby affecting the macroscopic mechanical response. Omar et al. [9] highlighted the importance of fibre–matrix interactions in natural-rubber composites reinforced with plant fibres. Li et al. [10] further demonstrated that polymer-network organization and constituent interactions can significantly influence the mechanical response of natural-rubber-latex-based composites.

3.2.3. Latex density

The latex density was determined from three independent measurements, which yielded values of 1.0006, 1.0116, and 1.0156 g/cm³. The corresponding standard deviation was approximately 0.0076 g/cm³, indicating a relatively low dispersion among the three measurements. This limited variability suggests good consistency of the latex density under the experimental conditions. Such consistency is favourable for process reproducibility, as substantial density variations could reflect differences in latex composition or solids distribution and potentially contribute to non-uniform matrix impregnation within the textile reinforcement.

Taken together, the total solids content (46.9%), dynamic viscosity (1.14 mPa·s), and mean density (1.0093 g/cm³) indicate that the natural-rubber latex exhibited physical characteristics compatible with its use as the continuous matrix phase of a composite reinforced with a woven lignocellulosic textile preform. In particular, the relatively low viscosity is expected to facilitate latex penetration into the inter-fibre and inter-yarn spaces of the woven reinforcement prior to drying, thereby promoting matrix continuity throughout the composite architecture.

3.3. Textile architecture of the okra-fibre reinforcement

Figure 7 show the resulting fabric exhibited a bidirectional architecture consisting of parallel warp elements and perpendicular weft elements arranged in a plain-weave structure.

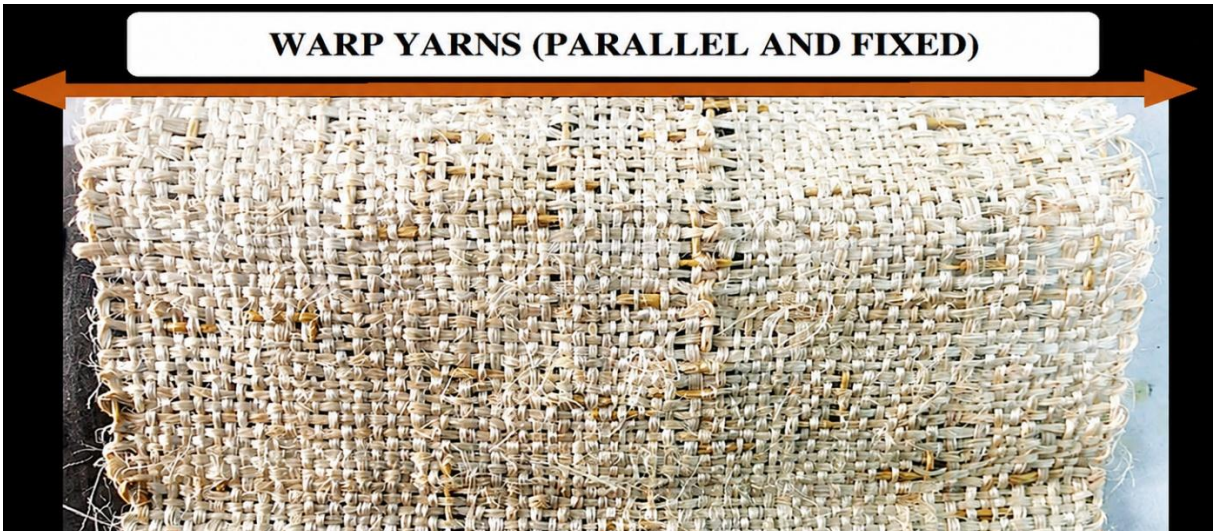


Figure 7. *Schematic illustration of the warp–weft interlacing architecture of the woven okra-fibre reinforcement.*

The main advantage of this architecture is the creation of a continuous reinforcement network within the plane of the material. The interlacing points restrict relative movement between the constituent elements and provide dimensional stability to the preform before and during impregnation. However, the textile architecture also modifies the load path. The weft elements do not remain perfectly straight; instead, they follow an undulating trajectory resulting from their alternating passage over and under the warp elements. This undulation, characterized by a 12% crimp, causes the fibres to deviate from the macroscopic loading direction. Korkmaz et al. [3] demonstrated that reinforcement architecture influences stress-transfer mechanisms and the mechanical response of woven composites. Kar et al. [4] likewise showed that the configuration of plant-fibre-based woven reinforcements can significantly affect the mechanical and thermal properties of polymer composites.

The okra-fibre fabric should therefore be regarded not simply as an assembly of cords, but as a reinforcement architecture in its own right, in which geometry controls stability, permeability and load-transfer efficiency.

3.3.1. Architectural parameters

The measured architectural parameters are presented in Table 5.

Table 5. *Architectural parameters*

Parameter	Value	Unit

Warp density	2.33	yarns·cm^{-1}
Weft density	1.83	yarns·cm^{-1}
Binding ratio	0.50	–
Weft crimp	12	%
Warp cover factor	0.186	–
Weft cover factor	0.146	–
Total cover factor	0.332	–
Fabric porosity	0.668	–
Contact-point density	4.26	contacts·cm^{-2}
Fibre volume fraction	0.30	–

The warp density (2.33 yarns·cm^{-1}) is higher than the weft density (1.83 yarns·cm^{-1}), indicating a slight asymmetry between the two principal directions of the fabric. The total cover factor of 0.332 indicates that a substantial fraction of the textile structure remains occupied by interstitial spaces. From a composite-processing perspective, this feature may facilitate matrix access to the reinforcement. However, a distinction must be made between initial porosity that facilitates impregnation and residual porosity after consolidation. The former may enhance latex penetration, whereas the latter may act as a source of stress concentration. This distinction is critical for interpreting the mechanical performance of the final composite. Chowdhury and Summerscales [5] demonstrated that woven-fabric architecture simultaneously governs permeability, processability and mechanical response. The present results are consistent with this coupled relationship between architecture and composite performance. The 12% crimp should also be considered as a load-transfer parameter. Part of the initial deformation under tensile loading may correspond to the progressive straightening of the undulated elements before full reinforcement mobilisation. Consequently, reinforcement geometry can contribute to the difference between the intrinsic properties of the fibres and the properties measured at fabric scale.

Anas et al. [6] recently demonstrated that fabric structure and consolidation conditions significantly affect the mechanical behaviour of cellulose-based composites. These findings support the interpretation that the final performance of the present bio-composite is directly linked to the architecture of its textile preform.

3.4. Physical and mechanical properties of the okra-fibre fabric

The properties of the resulting fabric are summarized in Table 6.

Table 6. *Physical and mechanical properties of the okra-fibre fabric*

Property	Unit	Value
Mean thickness	mm	1.080
Areal density	g/m²	348.8
Elongation at break	%	3.456
Maximum stress	MPa	6.057
Apparent Young's modulus	MPa	77.640

The mean fabric thickness was 1.080 mm, while the areal density reached 348.8 g/m². These values indicate a preform containing a substantial amount of fibre material per unit area. The elongation at break of 3.456% indicates limited extensibility of the fabric. This response is consistent with the lignocellulosic nature of the reinforcement and the plain-weave architecture, which restricts global extension while allowing stress redistribution between the warp and weft systems. The maximum stress reached 6.057 MPa, while the apparent Young's modulus was 77.640 MPa. These values should not be interpreted as intrinsic properties of the elementary fibres. They represent the response of a complex textile architecture incorporating cord stiffness, twist, fibre orientation, interlacing interactions and crimp. The apparent modulus therefore results from a combination of structural mechanisms. Pervaiz et al. [7] demonstrated that the architecture of natural-fibre fabrics strongly influences composite mechanical behaviour, with interlacing points and reinforcement orientation affecting stress transfer. For the present okra-fibre fabric, the plain-weave architecture therefore provides a balance between reinforcement stability, deformability and stress-transfer efficiency. Thickness and areal density are also important for composite manufacturing. An areal density of 348.8 g/m² represents a significant amount of reinforcement material to be impregnated. The matrix must therefore be sufficiently mobile and available to achieve effective coverage of the reinforcement.

This relationship between reinforcement architecture and impregnation is central to the design of the composite.

3.5. Fabrication of the latex–okra-fibre bio-composites

Figure 8 show the two formulations were produced from the okra-fibre fabric and natural rubber latex, distinguished by red and black coloration.

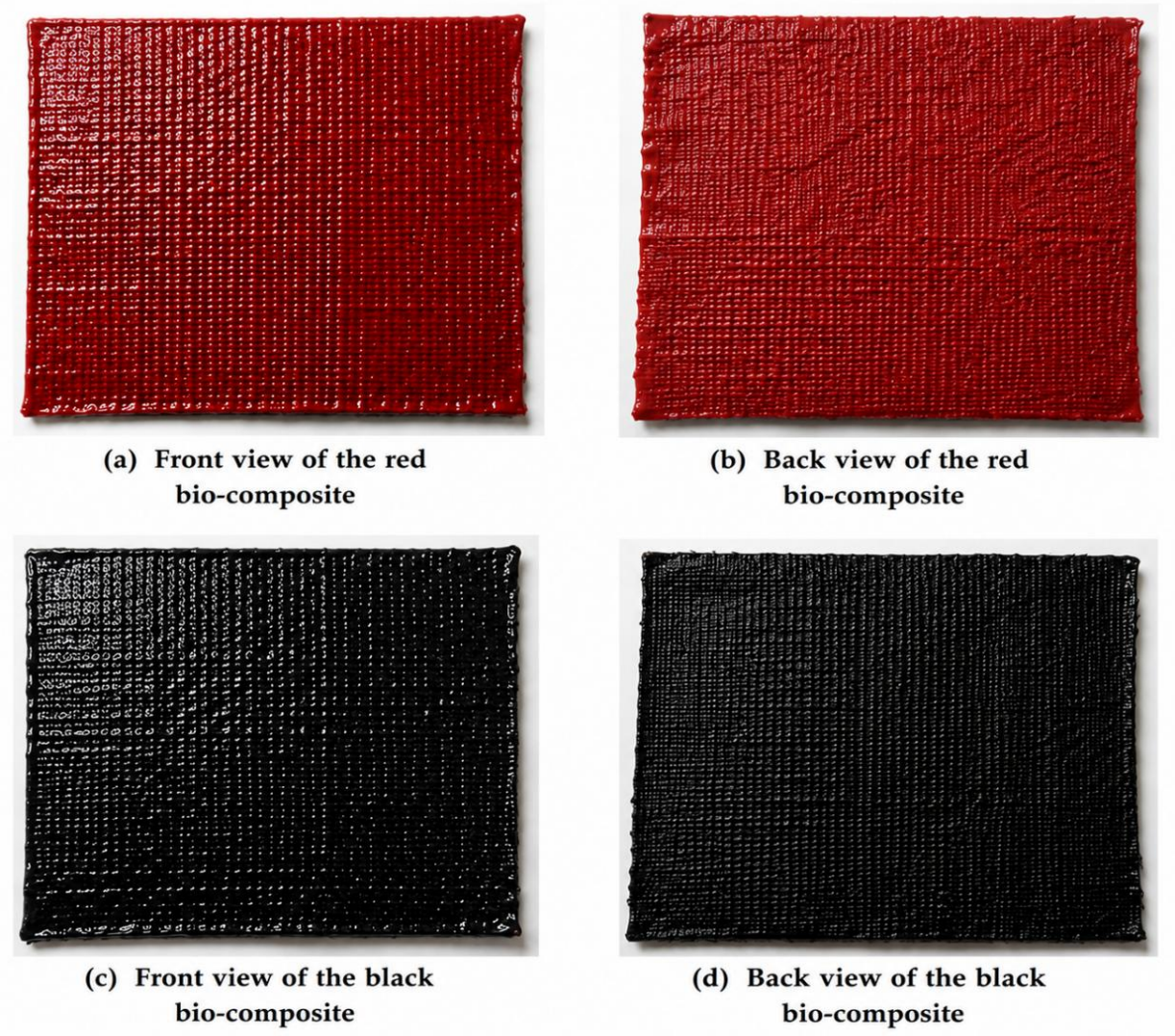


Figure 8. *Macroscopic appearance of the developed bio-composites: (a,b) front and back views of the red bio-composite; (c,d) front and back views of the black bio-composite.*

Macroscopic observations revealed continuous composite plates for both formulations, with the woven reinforcement embedded within the natural-rubber matrix. The observed macroscopic continuity provides preliminary evidence of successful impregnation and indicates that the latex was able to consolidate the reinforcement into a continuous composite structure. However, macroscopic observations alone cannot demonstrate the quality or strength of fibre–matrix interfacial bonding.

In fibre-reinforced composites, the mechanical response depends on effective stress transfer from the matrix to the reinforcement, which is influenced by interfacial contact, impregnation quality, reinforcement distribution, and the presence of local defects or voids. Omar et al. [9]

identified fibre–matrix interactions as an important factor governing the behaviour of natural-rubber composites reinforced with plant fibres. Li et al. [10] likewise demonstrated that polymer-network organization and constituent interactions can significantly influence the mechanical response of natural-rubber-latex-based composites.

The difference in coloration between the two formulations should therefore not be interpreted, by itself, as evidence of an intrinsic difference in mechanical performance. Instead, the red and black formulations should be compared on the basis of their experimentally determined mechanical, hydric, and environmental-ageing properties. Any formulation-dependent differences observed in these properties should subsequently be discussed in relation to the measured characteristics of the composite system, while avoiding attribution to specific interfacial or morphological mechanisms unless supported by dedicated characterization.

3.6. Morphological characterization of the bio-composites by SEM

Ramachandran *et al.* reported that fibre–matrix compatibility is a key factor controlling stress transfer and the mechanical performance of natural-fibre composites [14]. Mohammed *et al.* similarly emphasized the importance of interfacial bonding in determining the efficiency of load transfer between natural fibres and polymer matrices [22]. These considerations are relevant to the present bio-composites, which exhibit distinct morphological features in the SEM observations.

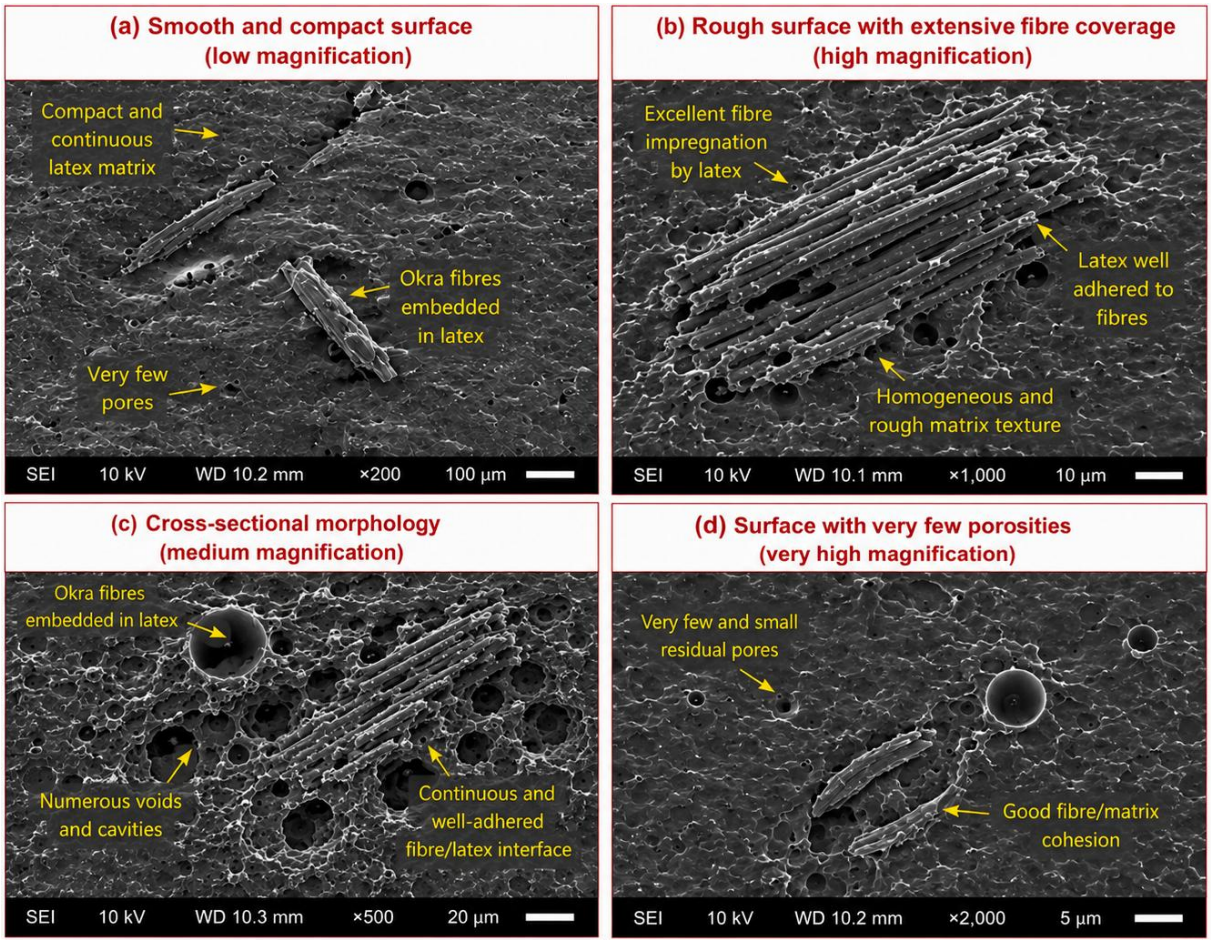


Figure 9. *SEM micrographs of the red-dyed okra-fibre/natural-latex bio-composite at different magnifications: (a) smooth and compact surface at low magnification (×200); (b) rough surface showing extensive fibre coverage by the latex matrix at high magnification (×1,000); (c) cross-sectional morphology showing the fibre–latex interface (×500); and (d) local surface morphology with low apparent porosity at very high magnification (×2,000). SEM observations were performed in secondary electron imaging (SEI) mode at an accelerating voltage of 10 kV, with working distances of 10.1–10.3 mm.*

The red bio-composite exhibits a relatively smooth and compact morphology, with substantial fibre embedment within the latex matrix (Figure 9). The matrix appears comparatively continuous around the fibres, while only a limited number of apparent pores are observed at high magnification. The cross-sectional morphology also suggests relatively continuous fibre–latex contact. In contrast, the black bio-composite displays a more heterogeneous morphology (Figure 10), characterized by locally exposed fibres, incomplete impregnation, micro-cavities, and apparent discontinuities at the fibre–latex interface. At high magnification, residual pores and localized matrix cracking or fibre–matrix separation are also visible.

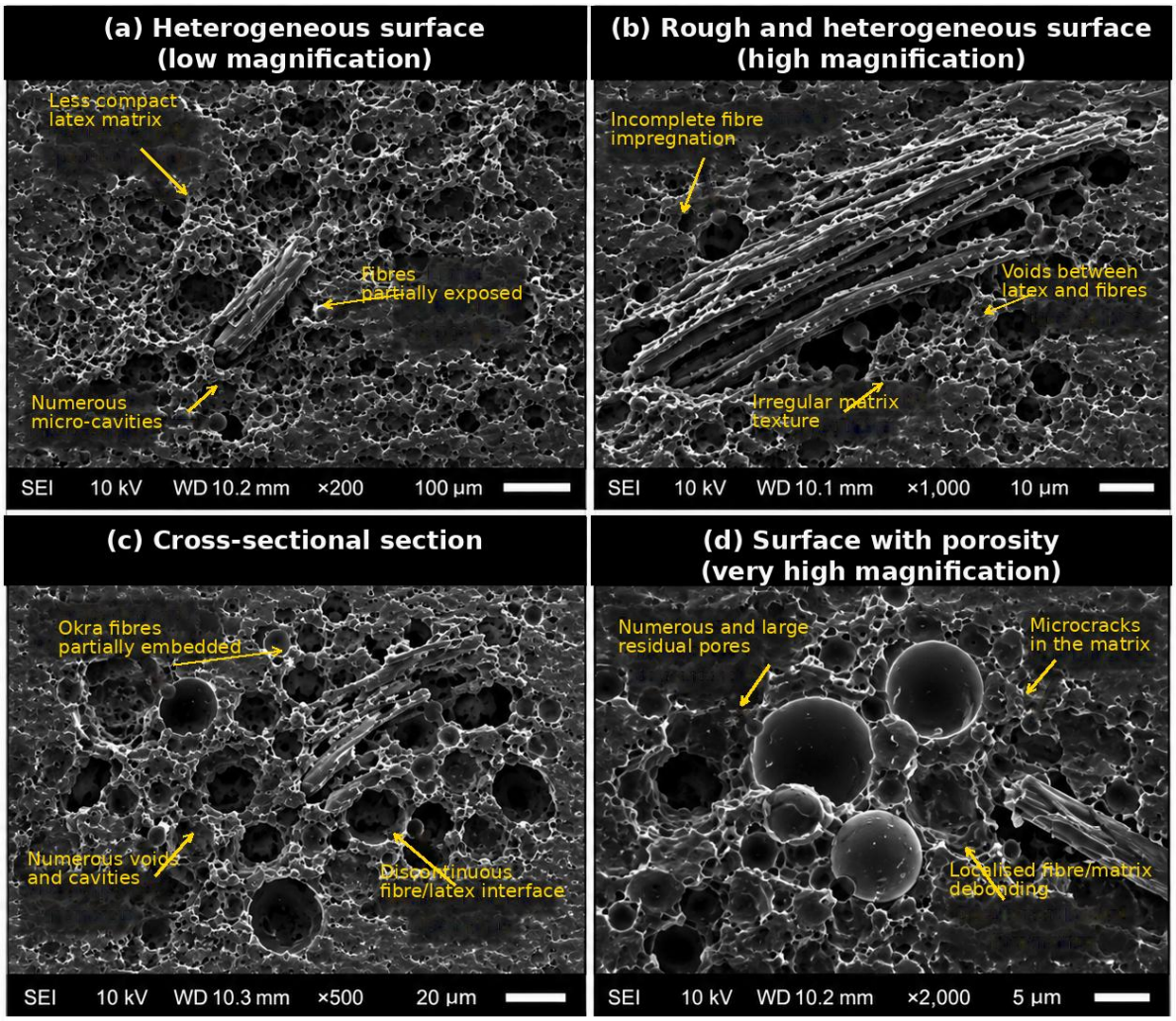


Figure 10. *SEM micrographs of the black okra-fibre/natural-latex bio-composite at different magnifications: (a) heterogeneous surface at low magnification (×200), showing a relatively non-compact latex matrix, numerous micro-cavities, and partially exposed fibres; (b) rough and heterogeneous surface at high magnification (×1,000), showing incomplete fibre impregnation, voids between the latex matrix and fibres, and an irregular matrix texture; (c) cross-sectional morphology at ×500, showing partially embedded okra fibres, numerous voids and cavities, and a discontinuous fibre–latex interface; and (d) surface morphology at very high magnification (×2,000), showing numerous and relatively large residual pores, matrix microcracks, and localized fibre–matrix debonding. SEM observations were performed in secondary electron imaging (SEI) mode at an accelerating voltage of 10 kV, with working distances of 10.1–10.3 mm.*

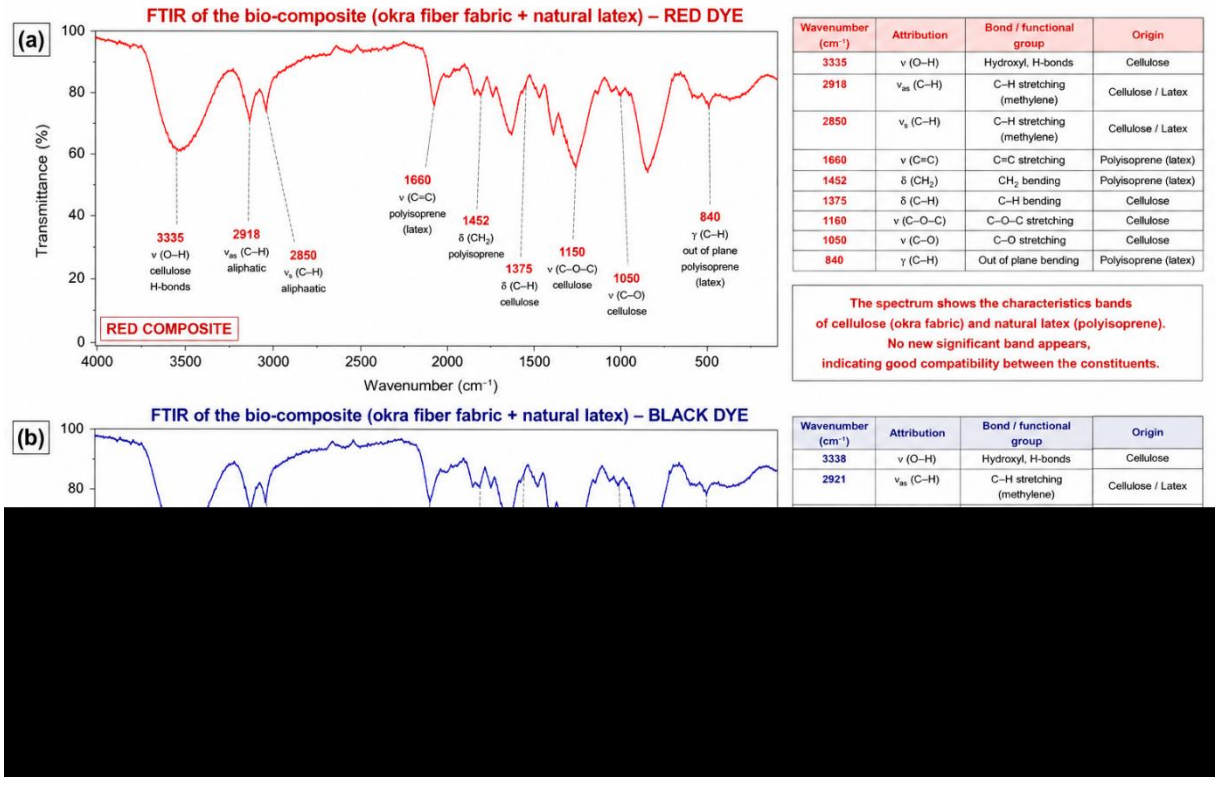
The comparison therefore suggests a more compact and continuous microstructure for the red formulation, whereas the black formulation exhibits a greater number of apparent morphological defects. Such defects can act as local stress-concentration sites and reduce the efficiency of stress transfer within natural-fibre composites [14]. Brodowsky and Hennig further demonstrated the importance of the fibre–matrix interphase in interfacial stress transfer [14].

This morphological difference is consistent with the tensile results. The red bio-composite exhibited a Young's modulus of 291.858 MPa and a maximum tensile stress of 11.907 MPa, compared with 155.412 MPa and 7.228 MPa, respectively, for the black formulation. The more compact morphology and greater apparent fibre embedment of the red formulation may therefore contribute to its higher stiffness and tensile strength.

However, SEM provides qualitative morphological evidence rather than a direct quantitative measurement of interfacial adhesion. The observed differences should consequently be considered together with the FTIR, XRD and TGA/DTG results to establish a more comprehensive structure–property relationship.

3.7. Fourier-transform infrared spectroscopy (FTIR) analysis

The FTIR spectra of the red- and black-dyed okra-fibre/natural-latex bio-composites are presented in Figure 11. Both spectra exhibit the characteristic absorption bands associated with the lignocellulosic okra fibres and the natural-latex matrix, confirming the coexistence of the two main constituents in the developed bio-composites.



Wavenumber (cm⁻¹)	Attribution	Bond / functional group	Origin
3335	ν (O–H)	Hydroxyl, H-bonds	Cellulose
2918	νas (C–H)	C–H stretching (methylene)	Cellulose / Latex
2850	νs (C–H)	C–H stretching (methylene)	Cellulose / Latex
1660	ν (C=C)	C=C stretching	Polyisoprene (latex)
1452	δ (CH2)	CH2 bending	Polyisoprene (latex)
1375	δ (C–H)	C–H bending	Cellulose
1160	ν (C–O–C)	C–O–C stretching	Cellulose
1050	ν (C–O)	C–O stretching	Cellulose
840	γ (C–H)	Out of plane bending	Polyisoprene (latex)

Wavenumber (cm⁻¹)	Attribution	Bond / functional group	Origin
3338	ν (O–H)	Hydroxyl, H-bonds	Cellulose
2921	νas (C–H)	C–H stretching (methylene)	Cellulose / Latex

Figure 11. *FTIR spectra of the red- and black-dyed okra-fibre/natural-latex bio-composites: (a) red-dyed bio-composite; (b) black-dyed bio-composite.*

For the red bio-composite, the principal absorption bands are located at 3335, 2918, 2850, 1660, 1452, 1375, 1160, 1050 and 840 cm^{-1}. The broad band at 3335 cm^{-1} is assigned to O–H stretching vibrations associated with hydroxyl groups and hydrogen bonding in the cellulose-rich fibre phase. Bands around 2900 cm^{-1} are characteristic of C–H stretching vibrations in cellulosic materials [14]. The bands at 1160 and 1050 cm^{-1} are associated with C–O–C and C–O stretching vibrations of the cellulose structure [14]. The bands at 1660, 1452 and 840 cm^{-1} are characteristic of the polyisoprene phase of natural latex, corresponding respectively to C=C stretching, CH_2 deformation and vibrations associated with the cis-1,4-polyisoprene structure [14].

For the black bio-composite, the corresponding bands occur at 3338, 2921, 2852, 1662, 1454, 1377, 1158, 1052 and 842 cm^{-1}. The same principal spectral features are therefore retained after black-dye incorporation. The small variations in band positions, generally within approximately 5 cm^{-1}, indicate only minor changes in the local vibrational environment rather than the appearance of a new dominant functional group.

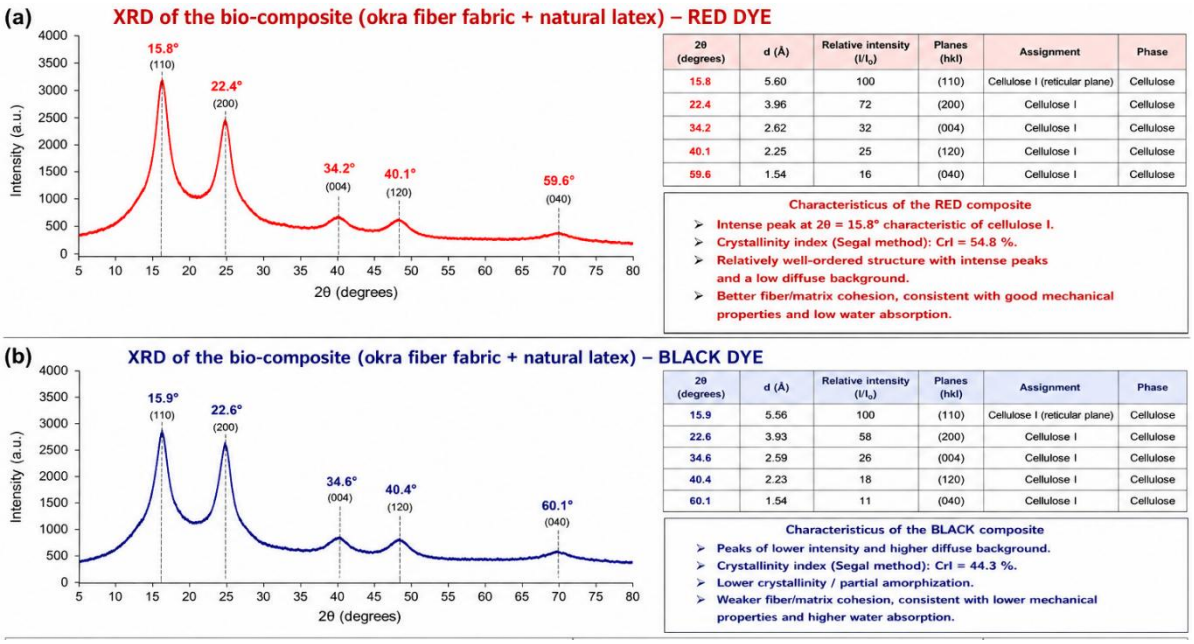
The comparison between the two formulations shows that no new major absorption band is observed in the black bio-composite. The characteristic cellulose- and polyisoprene-related bands remain present, indicating preservation of the main chemical signatures of the two constituents. The small shifts observed between the red and black formulations may therefore be associated with the presence of the dye and differences in the local chemical environment, rather than with the formation of a new major chemical structure.

Overall, the FTIR results confirm the coexistence of the lignocellulosic okra-fibre phase and the natural-latex (polyisoprene) phase in both bio-composites. The preservation of their characteristic absorption bands after dye incorporation suggests that the coloration process does not substantially modify the principal chemical functionalities of the composite. This result provides complementary evidence to the SEM observations and will be further considered together with the XRD and TGA/DTG results.

3.8. X-ray diffraction analysis of the bio-composites

The X-ray diffraction patterns of the red- and black-dyed okra-fibre/natural-latex bio-composites are presented in Figure 12. Both formulations exhibit diffraction features

characteristic of cellulose I, confirming that the crystalline structure of the lignocellulosic reinforcement is retained in the developed bio-composites. The main reflections are observed around 2θ = 15–16°, 22–23° and 34–35°, which are commonly associated with the crystalline domains of cellulose I [16].



2θ (degrees)	d (Å)	Relative intensity (I/I_0)	Planes (hkl)	Assignment	Phase
15.8	5.60	100	(110)	Cellulose I (reticular plane)	Cellulose
22.4	3.96	72	(200)	Cellulose I	Cellulose
34.2	2.62	32	(004)	Cellulose I	Cellulose
40.1	2.25	25	(120)	Cellulose I	Cellulose
59.6	1.54	16	(040)	Cellulose I	Cellulose

2θ (degrees)	d (Å)	Relative intensity (I/I_0)	Planes (hkl)	Assignment	Phase
15.9	5.56	100	(110)	Cellulose I (reticular plane)	Cellulose
22.6	3.93	58	(200)	Cellulose I	Cellulose
34.6	2.59	26	(004)	Cellulose I	Cellulose
40.4	2.23	18	(120)	Cellulose I	Cellulose
60.1	1.54	11	(040)	Cellulose I	Cellulose

Figure 12. *XRD patterns and main diffraction-peak characteristics of the red- and black-dyed okra-fibre/natural-latex bio-composites: (a) red-dyed bio-composite; (b) black-dyed bio-composite. The diffraction peaks are mainly assigned to cellulose I crystalline planes, with the Segal crystallinity index estimated at 54.8% for the red bio-composite and 44.3% for the black bio-composite.*

For the red bio-composite, the most intense diffraction peak occurs at 2θ = 15.8°, indexed as the (110) reflection, followed by the peak at 22.4°, assigned to the (200) plane of cellulose I. Additional reflections are observed at 34.2°, 40.1° and 59.6°, corresponding to the (004), (120) and (040) planes, respectively. The relatively pronounced intensity of the principal reflections and the comparatively low diffuse background indicate a substantial contribution of ordered cellulose domains.

The Segal crystallinity index (CrI) calculated from the diffraction profile is 54.8% for the red bio-composite. This value indicates that the material contains a significant crystalline cellulose fraction while retaining an amorphous contribution arising from the non-crystalline regions of the lignocellulosic reinforcement and polymeric matrix. The Segal approach is

widely used as an empirical estimation of cellulose crystallinity based on the relative intensity of the principal crystalline reflection and the amorphous contribution [16].

For the black bio-composite, the diffraction peaks are located at 15.9°, 22.6°, 34.6°, 40.4° and 60.1°, corresponding respectively to the (110), (200), (004), (120) and (040) planes. The positions of the principal reflections are therefore very close to those of the red formulation, indicating that the cellulose I crystalline polymorph is preserved after black-dye incorporation. However, the principal peaks exhibit lower relative intensities and the diffuse background is more pronounced.

The calculated CrI decreases to 44.3% for the black bio-composite, representing a difference of approximately 10.5 percentage points compared with the red formulation. This lower apparent crystallinity suggests a greater relative contribution of disordered regions in the black formulation. Similar XRD studies of lignocellulosic fibres have shown that changes in crystallinity can be associated with modifications of the relative proportions and organization of crystalline cellulose and amorphous constituents [16].

The higher CrI obtained for the red bio-composite is also consistent with its higher tensile stiffness and strength observed in the mechanical characterization. However, crystallinity should not be considered the sole determinant of mechanical performance. Kim and Lee demonstrated that parameters such as fibre aspect ratio, dispersion and alignment can influence the mechanical response of cellulose-based composite materials independently of crystallinity [16]. Therefore, the higher CrI of the red formulation should be interpreted together with the SEM observations, which showed a more compact matrix morphology and greater apparent fibre embedment.

Overall, the XRD results demonstrate that both bio-composites retain the cellulose I crystalline structure, while the red formulation exhibits a higher apparent crystallinity than the black formulation (54.8% versus 44.3%). The preservation of the same principal diffraction planes indicates that dye incorporation does not induce a detectable polymorphic transformation of the cellulose phase. The difference in CrI nevertheless suggests a difference in the relative organization of the crystalline and amorphous domains, which may contribute, together with the morphological and interfacial characteristics, to the different mechanical responses of the two formulations.

3.9. Thermal behaviour of the bio-composites by TGA/DTG

The TGA/DTG curves of the red- and black-dyed okra-fibre/natural-latex bio-composites are presented in Figure 13. Both formulations exhibit a multistage thermal degradation behaviour, reflecting the successive thermal responses of moisture and the different constituents of the lignocellulosic reinforcement and natural-latex matrix. Such multistage behaviour is characteristic of natural-fibre-reinforced composites, in which water loss is generally followed by the degradation of hemicellulose and cellulose and, at higher temperatures, the degradation of the polymeric matrix and residual carbonaceous structures [17].

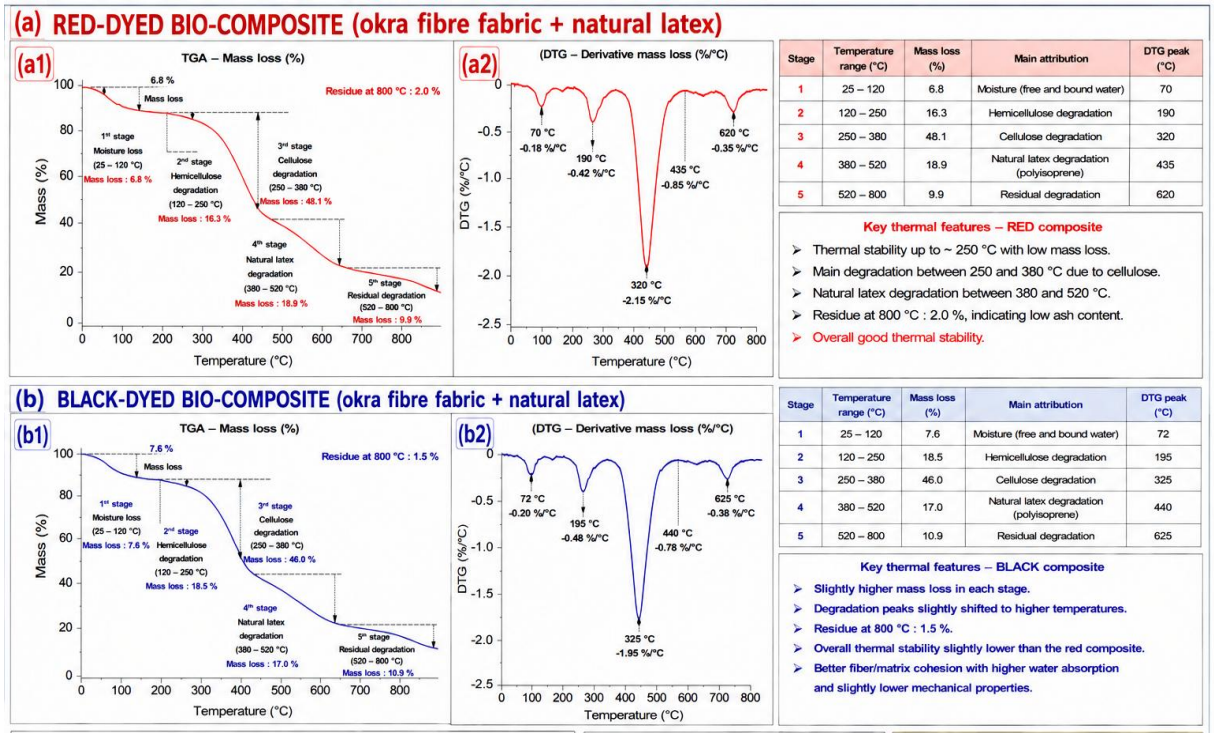


Figure 13. *TGA and DTG curves and main thermal degradation characteristics of the red- and black-dyed okra-fibre/natural-latex bio-composites: (a) TGA and DTG profiles of the red-dyed bio-composite; (b) TGA and DTG profiles of the black-dyed bio-composite.*

For the red bio-composite, the first mass-loss stage occurs between 25 and 120 °C, with a mass loss of 6.8% and a DTG maximum at 70 °C. This stage is mainly associated with the removal of free and bound moisture. The second stage, extending from 120 to 250 °C, corresponds to a further mass loss of 16.3%, with a DTG maximum at 190 °C, and is mainly associated with the degradation of thermally less stable lignocellulosic constituents, particularly hemicellulosic fractions. The major degradation occurs between 250 and 380 °C, where the red formulation loses 48.1% of its mass and exhibits its maximum DTG rate at 320

°C. This region is consistent with the principal decomposition of cellulose-rich structures in lignocellulosic materials [17].

A fourth degradation region is observed between 380 and 520 °C, with a mass loss of 18.9% and a DTG maximum at 435 °C. In the present composite, this region is attributed predominantly to the thermal degradation of the natural-latex phase, although contributions from residual lignocellulosic components cannot be completely excluded. Natural rubber is based mainly on cis-1,4-polyisoprene, whose thermal degradation occurs at relatively high temperatures compared with the more thermally sensitive lignocellulosic constituents [17].

For the black bio-composite, the same five-stage degradation pattern is observed. The first stage produces a mass loss of 7.6% between 25 and 120 °C, with a DTG maximum at 72 °C, followed by an 18.5% mass loss between 120 and 250 °C and a DTG maximum at 195 °C. The principal degradation stage extends from 250 to 380 °C, with a mass loss of 46.0% and a DTG maximum at 325 °C. The subsequent degradation of the latex-rich phase occurs between 380 and 520 °C, with a mass loss of 17.0% and a DTG maximum at 440 °C. The final residual degradation stage extends from 520 to 800 °C.

The comparison reveals an important distinction between the two formulations. The black bio-composite exhibits slightly higher DTG peak temperatures for the principal cellulose-related degradation and the high-temperature degradation stage, with shifts from 320 to 325 °C and from 435 to 440 °C, respectively. However, these higher peak temperatures should not be interpreted alone as evidence of superior overall thermal stability. The black formulation undergoes greater mass loss during the first two stages (7.6% and 18.5%) than the red formulation (6.8% and 16.3%), and its final residue at 800 °C is lower (1.5% versus 2.0%). Consequently, the thermal behaviour suggests slightly different degradation kinetics rather than a simple superiority of one formulation over the other.

Neto *et al.* emphasized that the thermal behaviour of natural-fibre composites depends on the nature and relative proportion of the fibre constituents, matrix, fibre treatment, processing conditions and other formulation parameters [17]. In the present case, the higher DTG temperatures observed for the black formulation may indicate a slightly delayed maximum rate of degradation, whereas the greater mass loss at lower temperatures indicates a larger fraction of thermally labile material being removed before the main degradation event. Therefore, the most appropriate interpretation is that the red formulation exhibits slightly

lower mass losses during the early stages and a higher final residue, while the black formulation exhibits slightly higher temperatures for the maximum degradation rates.

The 2.0% residue at 800 °C for the red formulation and 1.5% for the black formulation indicate that only a small fraction of the initial material remains after extensive thermal degradation under the experimental conditions. The residual fraction may include thermally stable inorganic components and carbonaceous residues generated during pyrolysis. The low residue values also suggest a relatively low inorganic/ash contribution to the investigated bio-composites, although an ash analysis would be required to quantify this contribution independently [17].

Overall, the TGA/DTG results demonstrate that both bio-composites possess a multistage thermal degradation profile, with the principal mass loss occurring in the cellulose-rich degradation region and a subsequent high-temperature degradation associated predominantly with the natural-latex phase. The red formulation shows lower early-stage mass losses and a slightly higher final residue, whereas the black formulation displays slightly higher DTG peak temperatures. These results indicate that the two dye formulations retain broadly comparable thermal degradation mechanisms, while exhibiting moderate differences in degradation kinetics and residual mass.

3.10. Colorimetric characteristics of the bio-leathers

The colourimetric characteristics of the developed black and red bio-leathers were evaluated using the **CIE L*a*b*** colour space. The measured colour coordinates are presented in **Figure 13**. The CIELAB system provides three independent parameters describing lightness (**L***), the green–red axis (**a***), and the blue–yellow axis (**b***), and is widely used for quantitative colour characterization of textile and related materials [18].

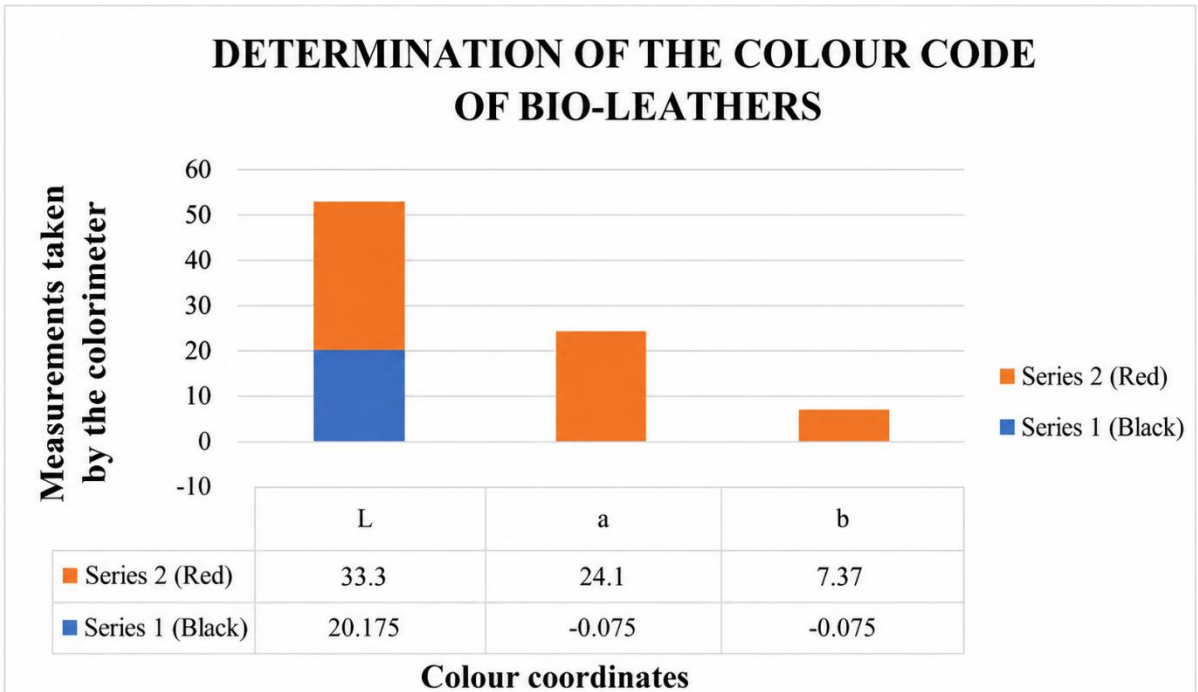


Figure 13. *CIE L*a*b* colour coordinates of the black and red bio-leathers.*

As shown in Figure 13, the **black bio-leather (Series 1)** exhibited a low lightness value of **L* = 20.175**, with a* and b* coordinates of **−0.075** and **−0.075**, respectively. The values of a* and b* close to zero indicate that the chromatic contribution is very limited, whereas the low L* value is consistent with the dark appearance of the material [18].

The **red bio-leather (Series 2)** exhibited a higher lightness value of **L* = 33.3**, together with a strongly positive **a*** value of **24.1**. This positive a* coordinate indicates a pronounced shift toward the red region of the CIELAB colour space. Its **b*** value of **7.37** indicates a moderate contribution toward the yellow direction. Consequently, the red formulation exhibits a substantially different chromatic profile from the black formulation.

The calculated colour difference between the two bio-leathers was **ΔE*ab ≈ 28.5**. The CIE 1976 ΔE*ab parameter represents the Euclidean colour difference between two positions in the CIELAB space; therefore, the high value obtained here indicates a **large and readily perceptible colour difference** between the two formulations [18].

The colour contrast is mainly associated with the substantial change in the **a*** coordinate, which shifts from approximately zero for the black bio-leather to **24.1** for the red formulation. Differences in L* and b* additionally contribute to the overall ΔE*ab value. These results demonstrate that the two bio-leather formulations possess **clearly differentiated and quantitatively measurable colour characteristics**, which is relevant when controlled colour appearance is required in the development of bio-based leather-like materials.

3.6. Mechanical and functional properties of the bio-composites

The properties measured for the two formulations are presented in Table 7.

Table 7. *Properties of the latex–okra-fibre bio-composites*

Property	Black bio-composite	Red bio-composite
Young's modulus (MPa)	155.412	291.858

Elongation at break (%)	10.177	7.993
Maximum stress (MPa)	7.228	11.907
Moisture regain (%)	2.816	3.064
Water absorption (%)	28.236	22.259
Thickness (mm)	1.957	1.751
Areal density (g/m²)	1526.97	1537.07
Water impermeability (%)	100	100
Stress after water ageing (MPa)	2.971	2.900
Stress after humidity ageing (MPa)	5.060	2.720
Elongation after water ageing (%)	4.515	13.671
Elongation after humidity ageing (%)	21.112	4.181
Young's modulus after water ageing (MPa)	88.622	45.907
Young's modulus after humidity ageing (MPa)	**67.284**	**254.910**

The properties measured for the two bio-composite formulations are summarized in Table 5. The red formulation exhibited substantially higher stiffness and tensile strength than the black formulation, with Young's modulus increasing from 155.412 to 291.858 MPa (+87.8%) and maximum stress increasing from 7.228 to 11.907 MPa (+64.7%). This increase in stiffness and strength was accompanied by a reduction in elongation at break from 10.177% to 7.993% (−21.5%), indicating a clear stiffness–ductility trade-off associated with the formulation.

The red bio-composite also exhibited lower water absorption (22.259%) than the black formulation (28.236%), corresponding to a reduction of approximately 21.2%, whereas moisture regain remained relatively similar (3.064% for red versus 2.816% for black). Both formulations exhibited 100% water impermeability under the adopted spray-test conditions.

The differences observed between the two formulations indicate that coloration and/or formulation-related factors may influence the mechanical and hydric behaviour of the composite. However, the present measurements do not allow the specific contribution of

pigment dispersion, fibre–matrix interactions, or changes in matrix morphology to be isolated. These mechanisms should therefore be considered as possible explanations rather than experimentally demonstrated causes

3.6.1. Tensile response

The most significant result concerns the difference in mechanical response between the two formulations. The red bio-composite exhibited a Young's modulus of 291.858 MPa, compared with 155.412 MPa for the black bio-composite, corresponding to an increase of 87.8%. In parallel, the maximum stress increased from 7.228 MPa for the black composite to 11.907 MPa for the red composite, corresponding to an increase of 64.7%. This simultaneous increase in stiffness and strength is a significant result. It indicates that, under the investigated conditions, the red formulation enables more effective mobilisation of the load-bearing structure. However, this improvement is accompanied by a decrease in elongation at break from 10.177% to 7.993%, corresponding to a reduction of 21.5%. The mechanical response therefore shifts towards a stiffer and stronger, but less extensible, material. In a natural-rubber matrix composite, this behaviour can be interpreted in terms of stress transfer between the polymer matrix and the cellulosic reinforcement. Lozada et al. [12] showed that the mechanical properties of natural-rubber/cellulose composites are strongly influenced by reinforcement morphology and fibre–matrix interactions. The higher Young's modulus of the red formulation therefore suggests more effective reinforcement mobilisation under the present test conditions. Stress applied to the matrix may be transferred more efficiently to the fibre network, thereby increasing the apparent stiffness and tensile strength of the composite.

However, this interpretation should remain cautious. The available experimental data do not directly identify the mechanism responsible for the difference between the two formulations. No quantitative morphological or interfacial characterization is available to demonstrate that the red formulation possesses stronger interfacial adhesion. It would therefore be scientifically inappropriate to attribute the 87.8% increase in modulus directly to the red pigment. The results demonstrate a performance difference between the two formulations, but the underlying mechanism may involve several factors, including local matrix distribution, composite packing, pigment dispersion and fibre–matrix interactions.

This distinction between experimental observation and mechanistic interpretation is essential for the scientific analysis of the material.

3.6.2. Moisture and water behaviour

Moisture regain was 2.816% for the black composite and 3.064% for the red composite, corresponding to a relatively small difference of 8.8%. A more pronounced difference was observed in water absorption. Water absorption decreased from 28.236% for the black composite to 22.259% for the red composite, corresponding to a reduction of approximately 21.2%. This behaviour is particularly relevant because it occurs simultaneously with the increase in modulus and strength observed for the red formulation. Water absorption depends on several mechanisms, including the accessibility of hydrophilic regions of cellulose, interstitial volume, matrix distribution and the extent to which the fibres are encapsulated by the polymer. A more effective matrix coverage of the reinforcement could reduce the accessibility of some hydrophilic sites to water. Lozada et al. [12] demonstrated that the incorporation of cellulosic fibres into natural rubber simultaneously modifies mechanical properties and water-transport behaviour. The present results are consistent with this coupled relationship between reinforcement architecture, matrix and moisture response. The 100% water impermeability measured for both formulations is also a significant functional result. It indicates that, despite the initial porosity of the textile reinforcement, the latex matrix produced a macroscopically continuous water barrier under the experimental test conditions. This property is directly relevant to the intended application as a bag material, for which resistance to water penetration is an important functional requirement.

3.6.3. Thickness and areal density

The black composite exhibited a thickness of 1.957 mm, compared with 1.751 mm for the red composite, corresponding to a 10.5% reduction for the red formulation. The areal densities were 1526.97 g/m² and 1537.07 g/m², respectively, indicating very similar mass per unit area. This combination is relevant from a materials-engineering perspective: the red formulation exhibits lower thickness while maintaining a comparable areal density and simultaneously providing higher stiffness and strength. The thickness difference may reflect differences in matrix distribution or consolidation of the composite structure. However, the available data do not allow the mechanism responsible for this difference to be quantitatively established.

3.7. Effect of environmental ageing on mechanical performance

Ageing analysis provides insight into the stability of the developed bio-composites under aqueous and high-humidity exposure. After 30 days of water ageing, the maximum tensile stress decreased to 2.971 MPa for the black composite and 2.900 MPa for the red composite,

compared with initial values of 7.228 and 11.907 MPa, respectively. These values correspond to strength reductions of approximately 58.9% for the black composite and 75.6% for the red composite. The pronounced loss of tensile strength following water exposure demonstrates the sensitivity of the composite system to aqueous conditions.

This reduction may be associated with moisture uptake by the lignocellulosic reinforcement and the resulting changes in the fibre–matrix system. Because cellulose-based fibres are intrinsically hydrophilic, water penetration can promote swelling and dimensional changes within the reinforcement and may modify the contact conditions between the fibres and the natural-rubber matrix. Such changes can affect stress-transfer efficiency and promote local interfacial discontinuities under tensile loading. In a composite combining a hydrophilic lignocellulosic reinforcement with an elastomeric matrix, the resulting moisture-induced structural changes may therefore contribute to the observed deterioration in tensile strength. This interpretation is consistent with previous observations concerning fibre–matrix interactions in natural-rubber/plant-fibre composites [9] and the behaviour of cellulose-reinforced natural rubber [13].

A markedly different response was observed after 30 days of high-humidity exposure at approximately 98% RH. The maximum tensile stress reached 5.060 MPa for the black composite, compared with 2.720 MPa for the red composite. Thus, under this particular ageing condition, the black formulation retained a higher tensile strength than the red formulation. This behaviour contrasts with the initial mechanical ranking, for which the red composite exhibited substantially higher strength. The result therefore demonstrates a formulation-dependent reversal in mechanical performance under environmental exposure.

The different response of the two formulations is also evident from the deformation behaviour. Following water ageing, the elongation at break was 4.515% for the black composite and 13.671% for the red composite. After high-humidity ageing, the corresponding values were 21.112% and 4.181%, respectively. The black composite therefore exhibited a pronounced increase in deformability under high-humidity exposure, whereas the red composite retained a substantially more constrained deformation response.

The Young’s modulus further highlights this formulation-dependent response. After water ageing, the modulus decreased to 88.622 MPa for the black composite and 45.907 MPa for the red composite. Following high-humidity ageing, the modulus was 67.284 MPa for the black composite but remained considerably higher for the red composite, at 254.910 MPa.

Consequently, the black formulation exhibited higher retained tensile strength after high-humidity exposure, whereas the red formulation retained markedly greater stiffness. This result demonstrates that environmental ageing does not simply produce a uniform deterioration of all mechanical properties; rather, it modifies the balance between strength, stiffness, and deformability in a formulation-dependent manner.

The observed behaviour indicates that the environmental response of the developed bio-composites is governed by the combined effects of reinforcement architecture, elastomeric matrix behaviour, moisture exposure, and fibre–matrix interactions. The contrasting responses of the red and black formulations suggest that the factors controlling initial mechanical performance may differ from those governing mechanical retention after environmental exposure. However, the present experimental data do not allow the specific contribution of pigment dispersion, interfacial modification, matrix-network changes, or moisture-induced morphological effects to be isolated. These mechanisms should therefore be regarded as plausible interpretations requiring dedicated chemical, morphological, and interfacial characterization.

Importantly, the ageing study was performed at a single exposure duration of 30 days. The observed differences and the reversal in mechanical ranking should therefore be interpreted as timepoint-specific experimental observations rather than as evidence of a general degradation kinetic law. Further investigations involving multiple ageing durations would be required to establish degradation kinetics and determine whether the observed formulation-dependent trends persist over longer exposure periods.

3.8. Positioning of the bio-composite relative to reference materials

The performance of the two formulations was compared with several materials used or proposed for leather goods and bag applications. The comparison data reported in the manuscript are presented in Table 8.

Table 8. *Comparison of the developed bio-composites with selected materials used in leather goods*

Material	Young's modulus (MPa)	Strength (MPa)	Elongation (%)	Water absorption (%)	Thickness (mm)
Black bio-composite	155.41	7.23	10.18	28.24	1.96

Red bio-composite	291.86	11.91	7.99	22.26	1.75
Bovine leather	30–100	15–35	30–70	10–20	1.5–2.5
Vegea®	20–70	8–25	20–60	15–28	1.0–2.0
Piñatex®	20–60	10–25	25–60	20–30	0.8–1.5
Desserto®	25–70	15–30	30–55	15–22	1.2–2.0
Mylo™	15–50	8–20	20–50	18–25	1.2–2.0
AppleSkin®	≈20–60	≈14	18–45	15–25	0.8–1.6
Mylea™	NR	8–11	22–35	NR	NR
SnapPap®	NR	24.9	7.5	10.3	NR
Teak Leaf®	NR	12.2	30.7	0.1	NR
Kombucha leather	NR	9.7	5.1	0.1	NR

The comparative data presented in Table X were obtained from Yizengaw et al. [11] and Oleksińska-Merida et al. [12]. The developed red bio-composite exhibited a Young's modulus of **291.86 MPa**, placing it above the stiffness ranges reported for the bio-based materials included in the comparison. This relatively high stiffness constitutes one of the notable mechanical characteristics of the developed composite.

However, the maximum tensile stress of the red bio-composite (**11.91 MPa**) remained below the highest values reported for several reference materials, particularly bovine leather, Desserto®, and SnapPap®. Accordingly, the developed material should not be considered universally superior to existing bio-based or commercial alternatives. Rather, its potential lies in the **combination of mechanical, hydric, and structural characteristics** achieved through the use of woven okra-fibre reinforcement and natural-rubber latex.

The red formulation exhibited a Young's modulus of **291.86 MPa**, a maximum tensile stress of **11.91 MPa**, an elongation at break of **7.99%**, a water absorption of **22.26%**, a thickness of **1.75 mm**, and **100% water impermeability** under the adopted spray-test conditions. This combination of relatively high stiffness, moderate tensile strength, limited elongation, and complete resistance to water penetration indicates potential for applications requiring dimensional stability and moisture protection.

The black bio-composite exhibited a different property profile, with lower tensile strength (**7.23 MPa**) and Young's modulus (**155.41 MPa**) but a higher elongation at break (**10.18%**). This comparatively greater deformability may be advantageous in applications where flexibility and compliance are more important than stiffness.

Nevertheless, comparisons with commercial and literature-based materials should be interpreted with caution. Reported properties can be strongly influenced by **material composition, reinforcement architecture, fibre or polymer content, processing conditions, specimen geometry, environmental conditioning, and testing standards**. Consequently, the values compiled in Table 6 should not be interpreted as a fully standardized one-to-one comparison.

The primary value of this comparison is therefore to position the developed latex–okra-fibre composites within the broader performance range of biosourced and bio-based materials and to highlight the **specific property combination** achieved by the present manufacturing route. In particular, the results suggest that the developed composites should be evaluated not solely on maximum tensile strength, but through a **multi-property perspective integrating stiffness, deformability, water resistance, density/thickness, and environmental stability**.

3.9. Process–structure–property–performance relationship

The complete set of results allows a multiscale interpretation of the behaviour of the developed bio-composite. At the first structural scale, the elementary okra fibres are grouped by twisting to produce a continuous cord. Twisting determines the cohesion, packing and porosity of the cord. At the mesoscale, the cords are organized into a plain-weave architecture. The fabric introduces additional structural parameters, including warp and weft densities, crimp, cover factors, contact-point density and fibre volume fraction. At the composite scale, the latex penetrates the accessible regions of the reinforcement and provides structural continuity. The characteristics of the latex particularly its total solids content, viscosity and density contribute to the effectiveness of this step. At the macroscopic scale, the combination of reinforcement and matrix produces the measured mechanical, hydric and environmental properties. The final performance is therefore the result of a hierarchical sequence of structural transformations:

elementary fibre → twisted cord → woven fabric → latex impregnation → fibre–matrix interface → composite → mechanical and functional performance.

This interpretation is particularly relevant for natural-fibre composites. Performance cannot be attributed solely to the chemical nature of the fibre or matrix; it also depends on reinforcement architecture and stress-transfer efficiency. The present results are consistent with the work of Rao et al. [1] on twisted structures, Korkmaz et al. [3] and Kar et al. [4] on reinforcement architecture, Chowdhury and Summerscales [5] on woven composite reinforcements, and Lozada et al. [12] on cellulose–natural-rubber interactions.

3.10. Trade-off between stiffness, strength, deformability and water behaviour

Comparison of the two formulations reveals a clear trade-off between the different properties. The red composite exhibits an 87.8% increase in Young's modulus and a 64.7% increase in strength, but a 21.5% reduction in elongation at break relative to the black composite. This evolution indicates that the improvement in load-bearing capability is accompanied by a reduction in extensibility. From a hydric perspective, the red formulation also exhibits a 21.2% reduction in water absorption. The red formulation therefore combines:

1. higher stiffness;
2. higher tensile strength;
3. lower elongation;
4. lower water absorption;
5. lower thickness;
6. identical water impermeability.

This profile makes it particularly attractive when the target function prioritizes dimensional stability and load-bearing capability. The black formulation, by contrast, provides greater elongation at break. It may therefore be considered when greater material flexibility is required. This distinction is important because it shows that the two formulations are not merely aesthetic variants of the same material: they exhibit different functional profiles. Nevertheless, the available results do not establish a direct causal relationship between the colourant and the observed performance differences. Additional characterization of morphology, pigment dispersion and fibre–matrix interfaces would be required to isolate this effect.

3.11. Potential of the bio-composite for multifunctional bag applications

The results demonstrate the feasibility of converting woven okra fibres into a continuous natural-rubber-based textile composite with properties relevant to multifunctional bag applications. The red formulation exhibits the most favourable initial mechanical profile for structural applications, with a Young's modulus of 291.86 MPa, maximum tensile stress of 11.91 MPa, elongation at break of 7.99%, water absorption of 22.26%, thickness of 1.75 mm, and 100% water impermeability. In comparison, the black formulation exhibits a Young's modulus of 155.41 MPa, maximum tensile stress of 7.23 MPa, and elongation at break of 10.18%, indicating a comparatively more compliant and extensible material.

From an application perspective, these characteristics suggest that the developed bio-composites could serve as structural and protective components of multifunctional bags, particularly where a combination of mechanical support, flexibility and resistance to water penetration is required. The higher stiffness and tensile strength of the red formulation are advantageous for maintaining dimensional stability and resisting mechanical loading, whereas the higher elongation of the black formulation may be beneficial where greater deformation capacity is required. The two formulations therefore offer different performance profiles rather than a simple hierarchy of material suitability.

The potential application is further supported by the multiscale characterization. SEM observations showed a relatively compact morphology and greater apparent fibre embedment for the red formulation, whereas the black formulation exhibited more heterogeneous morphology, residual pores and localized fibre–matrix discontinuities. These features are consistent with the observed difference in tensile performance. FTIR analysis confirmed the coexistence of the lignocellulosic fibre and natural-latex phases in both formulations, while XRD showed preservation of the cellulose I crystalline structure, with apparent crystallinity indices of 54.8% for the red formulation and 44.3% for the black formulation. The TGA/DTG results further demonstrated that both materials possess a multistage thermal degradation behaviour, indicating that the composite structure remains thermally stable over a range of temperatures before undergoing the principal degradation processes of the lignocellulosic and latex constituents.

Nevertheless, the ageing results constitute an important limitation for direct long-term application. The initial mechanical advantage of the red formulation was not fully retained

after environmental exposure, particularly after water ageing. Both formulations experienced substantial changes in tensile and deformation properties following ageing, demonstrating that environmental durability cannot be inferred solely from the initial mechanical performance.

Consequently, the developed bio-composite should presently be regarded as a promising candidate material for multifunctional bag components rather than as a fully validated commercial bag material. Further development should focus on improving fibre–matrix interfacial stability, optimizing latex impregnation, reducing residual voids and improving the moisture resistance of the lignocellulosic reinforcement. Additional cyclic ageing, flexural, tear, abrasion, seam and repeated-loading tests would also be necessary to establish the durability of the material under realistic bag-use conditions.

3.12. General discussion and scientific contribution

The present study demonstrates the feasibility of transforming extracted okra (*Abelmoschus esculentus*) bast fibres into a woven reinforcement and subsequently into a natural-rubber-latex composite through a hierarchical processing route involving fibre assembly, twisting, weaving, and latex impregnation. At the reinforcement level, the twisted cords exhibited a breaking stress of 38.2 MPa, a tenacity of 5.0 cN/tex, and a porosity of 34.5%, while the woven preform exhibited a total cover factor of 0.332, a crimp of 12%, and a fibre volume fraction of 0.30. These characteristics enabled the formation of a textile preform suitable for latex impregnation.

The complementary morphological, chemical, structural and thermal analyses provide a coherent interpretation of the formulation-dependent behaviour. SEM observations revealed a comparatively compact morphology for the red formulation, with greater apparent fibre embedment and fewer visible pores, whereas the black formulation exhibited locally exposed fibres, incomplete impregnation, micro-cavities and apparent fibre–matrix discontinuities. These morphological differences are consistent with the higher stiffness and tensile strength measured for the red formulation, although SEM provides qualitative rather than quantitative evidence of interfacial adhesion.

The FTIR spectra confirmed the coexistence of the lignocellulosic and natural-latex phases in both formulations. The red composite exhibited characteristic bands at 3335, 2918, 2850, 1660, 1452, 1375, 1160, 1050 and 840 cm^{-1}, while the corresponding bands for the black composite occurred at 3338, 2921, 2852, 1662, 1454, 1377, 1158, 1052 and 842 cm^{-1}. The small shifts, generally below approximately 5 cm^{-1}, and the absence of a new dominant

absorption band indicate that dye incorporation did not substantially modify the principal chemical functionalities of the composite system.

The XRD results further showed that both formulations retained the characteristic cellulose I crystalline structure. The principal reflections occurred around 2θ = 15–16°, 22–23° and 34–35°. The calculated apparent crystallinity index was 54.8% for the red composite and 44.3% for the black composite, corresponding to a difference of approximately 10.5 percentage points. The higher apparent crystallinity of the red formulation is consistent with its higher initial stiffness and tensile strength, but crystallinity alone cannot account for the mechanical differences because morphology, fibre organization and matrix distribution also contribute to the composite response.

The TGA/DTG analysis revealed multistage thermal degradation for both formulations. For the red composite, the principal degradation region occurred between 250 and 380 °C, with a mass loss of 48.1% and a DTG maximum at 320 °C, followed by a latex-dominated degradation region between 380 and 520 °C, with a DTG maximum at 435 °C. The black composite exhibited corresponding DTG maxima at 325 °C and 440 °C. Although these slightly higher peak temperatures indicate differences in degradation kinetics, they do not demonstrate superior overall thermal stability of the black formulation, which showed greater mass losses during the early degradation stages and a lower final residue (1.5% versus 2.0% for the red composite).

At the macroscopic level, these multiscale observations are consistent with the measured functional properties. Both formulations exhibited 100% water impermeability, while the red composite showed the highest initial stiffness and strength, with a Young's modulus of 291.858 MPa and a maximum stress of 11.907 MPa, compared with 155.412 MPa and 7.228 MPa, respectively, for the black composite. The red formulation also exhibited lower water absorption (22.259% versus 28.236%).

However, environmental ageing demonstrated that this initial advantage was not universally maintained. After 30 days of water exposure, tensile strength decreased by approximately 58.9% for the black composite and 75.6% for the red composite. Under high-humidity exposure, the black formulation retained higher tensile stress (5.060 MPa versus 2.720 MPa), whereas the red formulation retained substantially higher Young's modulus (254.910 MPa versus 67.284 MPa). Thus, environmental exposure modified the balance between strength,

stiffness and deformability and reversed the initial tensile-strength ranking under high-humidity conditions.

Taken together, the results establish a processing–structure–property–environment relationship for the woven okra-fibre/natural-latex composite. The processing route determines the hierarchical textile architecture; SEM reveals formulation-dependent morphological differences; FTIR confirms preservation of the principal chemical functionalities; XRD demonstrates retention of the cellulose I structure with different apparent crystallinity levels; TGA/DTG reveals differences in thermal degradation behaviour; and the mechanical, hydric and ageing results demonstrate the resulting macroscopic performance. The differences between the red and black formulations should nevertheless be interpreted as experimentally observed formulation-dependent effects, rather than as direct evidence of a dye-specific mechanism, because pigment dispersion and interfacial contributions were not independently quantified.

Overall, the scientific contribution of this work lies in integrating textile processing, multiscale characterization and environmental ageing within a single okra-fibre/natural-latex composite system. The material therefore represents a promising biosourced platform for flexible textile applications requiring water resistance, while its sensitivity to environmental exposure remains a significant limitation. Further research should focus on isolating the mechanisms responsible for the formulation-dependent response and on establishing ageing kinetics through multiple exposure durations and statistically replicated experiments.

4. Conclusion

This study established a low-technology processing route for converting okra (*Abelmoschus esculentus*) bast fibres into a woven natural-rubber-latex composite through sequential twisting, plain weaving, and latex impregnation. The results demonstrate the feasibility of transforming the extracted fibres into a cohesive textile reinforcement and subsequently into a continuous composite structure.

The twisted okra-fibre cords exhibited sufficient cohesion and tenacity (5.0 ± 0.3 cN/tex) for weaving, while the resulting plain-weave fabric provided a stable preform with an areal density of 348.8 g/m² and a total cover factor of 0.332. The natural-rubber latex, with a total solids content of 46.9% and a viscosity of 1.14 mPa·s, enabled the production of red and black composites exhibiting 100% water impermeability under the adopted test conditions.

The two formulations exhibited distinct initial mechanical and hydric behaviours. Compared with the black composite, the red formulation showed an 87.8% higher Young's modulus, a 64.7% higher maximum stress, a 21.5% lower elongation at break, and a 21.2% lower water absorption. These differences demonstrate that formulation is associated with substantial variations in composite performance. However, the present results do not establish a direct causal effect of the dye itself, since pigment dispersion, matrix distribution and fibre–matrix interactions were not independently isolated.

Environmental ageing further demonstrated that the initial performance ranking was not maintained under all exposure conditions. After 30 days of high-humidity exposure, the black composite retained a higher maximum stress, whereas the red formulation retained substantially higher stiffness. Water exposure resulted in pronounced tensile-strength losses of approximately 58.9% for the black composite and 75.6% for the red composite. These findings demonstrate that as-produced mechanical properties alone are insufficient to assess the performance of the material under environmental exposure.

Overall, the study demonstrates the potential of woven okra-fibre/natural-latex composites as biosourced materials for flexible textile applications requiring water resistance, while identifying environmental ageing as an important limitation. The combined processing, mechanical, hydric and structural characterization provides a basis for further optimization of the material system. Future research should focus on clarifying the mechanisms underlying the formulation-dependent behaviour, improving fibre–matrix interfacial stability, and evaluating multiple ageing durations with adequate statistical replication to establish degradation kinetics and long-term performance.

5-Funding declaration

The authors received no specific funding for this work.

6-Conflict of Interest

The authors declare that they have no conflict of interest.

7-Data Availability Statement

The data supporting the findings of this study are available from the corresponding author upon reasonable request.

8- Ethics approval, consent to participate, and consent to publish

Not applicable

[1] N. R. Nkoulou Nkoulou, S. Bassok, P. Etouke Owoundi, S. E. Ndjakomo, and J. Mbihi, "Influence of biological, chemical, and combined extraction methods on the physicochemical, structural, and mechanical properties of okra (*Abelmoschus esculentus*) fibers for natural latex-based bio-composite reinforcement," *Processes*, vol. 14, no. 15, Art. no. 2440, 2026, doi: 10.3390/pr14152440.

[2] Y. Rao, Z. Chen, N. Wei, T. Xiong, and K. Wang, "A hierarchical analytical model for twisted yarn reinforced plant fiber composites considering dual-scale filler content, porosity and local aggregation effect," *Composites Structures*, vol. 313, Art. no. 116928, 2023, doi: 10.1016/j.compstruct.2023.116928.

[3] Maidina, F. Muslim, Sudarmanto, D. Purnomo, A. Sumarno, and H. Purnomo, "Experimental investigation on tensile strength of twisted ramie fiber yarns," *Key Engineering Materials*, vol. 963, pp. 119–124, 2023, doi: 10.4028/p-sbxzF0.

[4] M. Korkmaz, R. Karakuzu, A. R. Labanieh, and F. Boussu, "The low velocity impact properties of three-dimensional warp interlock woven composites according to the fabric architecture," *Journal of Composite Materials*, vol. 58, no. 24, pp. 2655–2668, 2024, doi: 10.1177/00219983241266931.

[5] S. Kar, S. Pattnaik, and M. K. Sutar, "Assessment of mechanical and thermal properties of hybrid co-woven biofiber polymer composites," *Industrial Crops and Products*, vol. 222, Art. no. 119756, 2024, doi: 10.1016/j.indcrop.2024.119756.

[6] I. R. Chowdhury and J. Summerscales, "Woven fabrics for composite reinforcement: A review," *Journal of Composites Science*, vol. 8, no. 7, Art. no. 280, 2024, doi: 10.3390/jcs8070280.

[7] M. S. Anas, B. Ungerer, H. Al-Musawi, and U. Müller, "Regenerated cellulose as a sustainable alternative to glass fiber composites: Effects of fabric structure and applied pressure during curing," *Cellulose*, 2025, doi: 10.1007/s10570-025-06498-8.

[8] A. Pervaiz, F. Azam, A. Ahmad, F. Ahmad, S. Ahmad, T. Ullah, Y. Nawab, and K. Shaker, "An investigation of static and dynamic mechanical properties of eco-friendly textile PLA composites reinforced by flax woven fabrics," *International Journal of Polymer Science*, vol. 2024, Art. no. 2821777, 2024, doi: 10.1155/ijps/2821777.

[9] M. F. Omar, F. Ali, M. S. Jami, A. S. Azmi, F. Ahmad, M. Z. Marzuki, S. K. Muniyandi, Z. Zainudin, and M. P. Kim, "A comprehensive review of natural rubber composites: Properties, compounding aspects, and renewable practices with natural fibre reinforcement," *Journal of Renewable Materials*, vol. 13, no. 3, pp. 497–538, 2025, doi: 10.32604/jrm.2024.057248.

[10] S. Li, F. Liang, J. Zhou, and B. Shi, "Bio-inspired dual crosslinked network mediated by plant polyphenols for toughening natural rubber latex-based elastomeric composites," *Industrial Crops and Products*, vol. 210, Art. no. 118027, 2024, doi: 10.1016/j.indcrop.2024.118027.

[11] M. A. Yizengaw, A. A. Birlie, T. Tesfaye, R. Katrikan, E. B. Cheklie, and Z. Girma, "Grape waste as leather-like material alternative: A comprehensive review of ancient practices, current technologies, and future trends," *Journal of Renewable Materials*, vol. 14, no. 5, 2026, doi: 10.32604/jrm.2025.02025-0175.

[12] E. Oleksińska-Merida, M. Puchalski, and L. Herczyńska, "Bio-based and sustainable alternatives to conventional and synthetic leather," *Materials*, vol. 19, no. 6, Art. no. 1198, 2026, doi: 10.3390/ma19061198.

[13] E. R. Lozada, C. M. Gutiérrez Aguilar, J. A. Jaramillo Carvalho, J. C. Sánchez, and G. Barrera Torres, "Vegetable cellulose fibers in natural rubber composites," *Polymers*, vol. 15, no. 13, Art. no. 2914, 2023, doi: 10.3390/polym15132914.

[14] M. R. Sanjay, P. Madhu, M. Jawaid, P. Senthamaraikannan, S. Senthil, and S. Pradeep, "Characterization and properties of natural fiber polymer composites: A comprehensive review," *Journal of Cleaner Production*, vol. 172, pp. 566–581, 2018, doi: 10.1016/j.jclepro.2017.10.101.

[15] L. Segal, J. J. Creely, A. E. Martin, Jr., and C. M. Conrad, "An empirical method for estimating the degree of crystallinity of native cellulose using the X-ray diffractometer," *Textile Research Journal*, vol. 29, no. 10, pp. 786–794, 1959, doi: 10.1177/004051755902901003.

[16] N. M. Nurazzi, M. R. M. Asyraf, M. Rayung, M. N. F. Norrrahim, S. S. Shazleen, M. S. A. Rani, A. R. Shafi, H. A. Aisyah, M. H. M. Radzi, F. A. Sabaruddin, R. A. Ilyas, E. S. Zainudin, and K. Abdan, "Thermogravimetric analysis properties of cellulosic natural fiber polymer composites: A review on influence of chemical treatments," *Polymers*, vol. 13, no. 16, Art. no. 2710, 2021, doi: 10.3390/polym13162710.

[17] K. McLaren, "The development of the CIE 1976 (L* a* b*) uniform colour space and colour-difference formula," *Journal of the Society of Dyers and Colourists*, vol. 92, no. 9, pp. 338–341, 1976, doi: 10.1111/j.1478-4408.1976.tb03301.x.

Supplementary Files

This is a list of supplementary files associated with this preprint. Click to download.

- supplementsmaterials.zip